Electrochemical Analyses of Redox–Active Iron Minerals: A Review of Nonmediated and Mediated Approaches

3 **AUTHORS**, INCLUDING:

Michael Sander
ETH Zurich

43 PUBLICATIONS   **1,103** CITATIONS

Electrochemical Analyses of Redox-Active Iron Minerals: A Review of Nonmediated and Mediated Approaches

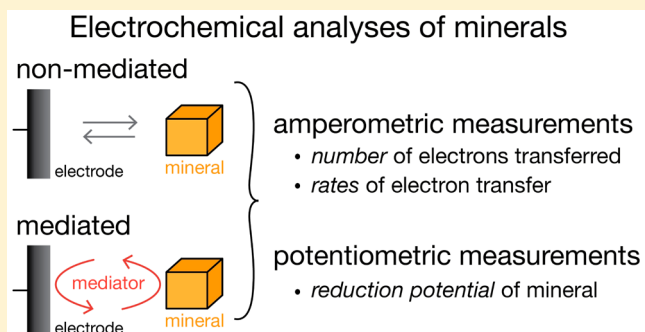Michael Sander,*[,†] Thomas B. Hofstetter,[‡] and Christopher A. Gorski*[,§]

[†]Department of Environmental Systems Science, Institute of Biogeochemistry and Pollutant Dynamics, Environmental Chemistry, Swiss Federal Institute of Technology (ETH), Universitätstrasse 16, 8092 Zurich, Switzerland

[‡]Environmental Chemistry, Swiss Federal Institute of Aquatic Science and Technology (Eawag), Ueberlandstrasse 133, 8600 Duebendorf, Switzerland

[§]Civil and Environmental Engineering, The Pennsylvania State University, 212 Sackett Building, University Park, Pennsylvania 16802-1408, United States

S *Supporting Information*

ABSTRACT: Redox-active minerals are ubiquitous in the environment and are involved in numerous electron transfer reactions that significantly affect biogeochemical processes and cycles as well as pollutant dynamics. As a consequence, research in different scientific disciplines is devoted to elucidating the redox properties and reactivities of minerals. This review focuses on the characterization of mineral redox properties using electrochemical approaches from an applied (bio)geochemical and environmental analytical chemistry perspective. Establishing redox equilibria between the minerals and working electrodes is a major challenge in electrochemical measurements, which we discuss in an overview of traditional electrochemical techniques. These issues can be overcome with mediated electrochemical analyses in which dissolved redox mediators are used to increase the rate of electron transfer and to facilitate redox equilibration between working electrodes and minerals in both amperometric and potentiometric measurements. Using experimental data on an iron-bearing clay mineral, we illustrate how mediated electrochemical analyses can be employed to derive important thermodynamic and kinetic data on electron transfer to and from structural iron. We summarize anticipated methodological advancements that will further contribute to advance an improved understanding of electron transfer to and from minerals in environmentally relevant redox processes.

Electrochemical analyses of minerals

non-mediated — amperometric measurements
- *number* of electrons transferred
- *rates* of electron transfer

mediated — potentiometric measurements
- *reduction potential* of mineral

■ INTRODUCTION

Redox-active minerals are ubiquitous in natural environments. Common redox-active elements in these minerals, besides oxygen and hydrogen, include iron, manganese, and sulfur. The redox properties and reactivities of these minerals have received considerable research interest in numerous scientific disciplines, including soil chemistry, biogeochemistry, environmental microbiology, environmental chemistry, and environmental engineering.[1−7] The broad interest reflects the fact that minerals play integral roles in a variety of electron transfer reactions that are important both for the biogeochemical cycling of elements and pollutant dynamics. For instance, redox transformations of iron-containing minerals are closely linked to the global carbon cycle. In anoxic soils and sediments, ferric (Fe^{3+})-containing minerals may serve as terminal electron acceptors during anaerobic microbial respiration on organic electron donors,[8−10] thereby contributing to organic carbon turnover in these systems. Microbial reduction of iron (oxyhydr-)oxides may also lead to their dissolution.[8,10−12] In this process, sequestered organic matter adsorbed to and/or enclosed in these minerals may become liberated and thereby susceptible to enhanced microbial degradation.[13−16] In the

context of pollutant dynamics, redox-active minerals may act as reductants (e.g., ferrous iron (Fe^{2+}) in oxides, sulfides, or clay minerals) or oxidants (e.g., Mn^{4+} in oxides) for organic and inorganic contaminants, including geogenic and anthropogenic metals and metalloids (e.g., lead, arsenic, chromium, uranium) as well as organic pollutants.[4,17−26]

Despite much interest, obtaining a thorough understanding of redox processes involving minerals has proven to be extremely challenging due to both conceptual and technical obstacles. Conceptually, electron transfer to and from minerals can involve concurrent processes that complicate interpretation. These processes include mineral dissolution, adsorption and complexation of dissolved redox-active elements onto the mineral surface, electron transfer from the adsorbed elements to redox-active elements in the mineral structure, electron conduction in the mineral structure, atom exchange, and mineral recrystallization reactions.[27−38] In the past two decades,

some of the conceptual complexities of mineral redox reactions have been understood and subsequently accounted for, thanks to considerable advances in spectroscopic and microscopic analyses. Today, a number of techniques are available to characterize mineral compositions and microstructures, including X-ray absorption near edge (XANES) and extended X-ray absorption fine structure (EXAFS) spectroscopy, X-ray diffraction, X-ray photoelectron spectroscopy, Mössbauer spectroscopy, (cryo-)transmission electron microscopy, calorimetry, and isotope ratio mass spectrometry.[39−44] The spectroscopic and microscopic insights are complemented by theoretical and computational improvements in describing mineral redox properties.[36,45−49] These advances led to the development of refined conceptual models that account for electron delocalization within mineral structures and the possibility for coupled redox reactions to occur at spatially separated sites.[28,29,50,51]

Compared to the significant advances in spectroscopic and microscopic tools and theory, considerably less progress has been made on improving experimental approaches to determine fundamental thermodynamic and kinetic parameters that describe mineral redox properties and reactivities in aqueous solutions. Instead, much of the current knowledge of mineral redox reactions is based on results from *indirect* measurements, such as measuring reaction rates and extents between iron-bearing minerals and organic probe compounds (e.g., substituted nitrobenzene compounds and chlorinated aliphatic compounds).[17,52−60] These indirect approaches have proven valuable for defining operational measures of mineral reactivity and/or redox buffering capacity and confirm many of the spectroscopically observed findings. These findings include reaction-induced irreversible alterations in the redox reactivity of minerals as well as the inability to describe redox-active minerals simply by single reduction potential values.[17,52−58] However, it is often difficult to determine the degree to which the observations depend on the probe compound(s) used. Furthermore, indirect measurements are often constrained in that they typically involve ex situ analyses and require relatively large mineral quantities and solution volumes. As a consequence, these measurements are ill suited to monitor changes in the redox states of minerals at high temporal resolution.

The constraints of indirect measurements can be overcome by using electrochemical approaches, which are capable of *directly* measuring kinetic and thermodynamic parameters of redox-active minerals in situ. Electrochemical approaches may also be used to follow changes in the redox states of minerals during reactions in real time. This review aims at familiarizing a larger audience in the fields of environmental sciences and biogeochemistry with analytical electrochemistry and its unique capabilities in characterizing redox-active minerals as well as other particulate geochemical phases. The review includes fundamental aspects of electrochemical techniques and is complemented by a detailed description of how to set up and carry out electrochemical measurements on redox-active minerals. The review is structured into four parts. The first provides a brief introduction to amperometric and potentiometric electrochemical measurements. The second part summarizes previous electrochemical work on mineral redox properties and highlights the major analytical challenges. The third and most extensive part of this review focuses on mediated electrochemical analyses of minerals. These analyses involve the use of dissolved redox mediators to facilitate redox

equilibration between the minerals and working electrodes in both amperometric and potentiometric measurements. In the fourth and final part we provide an outlook of anticipated methodological advances in mediated electrochemical analyses and highlight how the use of mediated electrochemical analyses in future studies will advance our understanding of electron-transfer processes involving particulate geochemical phases.

ELECTROCHEMICAL ANALYSES OF REDOX-ACTIVE MINERALS

Electrochemical techniques have unique capabilities for characterizing redox-active dissolved and solid-state geochemical phases with respect to both thermodynamics and kinetics of electron transfer.[61−65] Here, we briefly survey how electrochemical analyses are commonly conducted and what information they provide. We broadly split techniques between those in which electrons are exchanged between the sample and working electrode and currents are measured (i.e., amperometric techniques) and those in which no appreciable electron transfer occurs between the sample and working electrode and potentials are determined (i.e., potentiometric techniques). We further summarize challenges that arise when using these techniques to study redox-active minerals. For a comprehensive introduction to electrochemistry and electrochemical techniques, the reader is referred to several excellent textbooks and review articles on the topic.[61,65−70]

Amperometric Techniques. Amperometric techniques can be used to measure electron transfer to and from redox-active mineral phases under defined redox conditions. Amperometric measurements are typically conducted in three-electrode electrochemical cells that contain a working electrode, a reference electrode and a counter (or auxiliary) electrode.[67,71] The three electrodes are immersed into a solution, which is commonly pH-buffered and contains an electrolyte. A potentiostat is used to apply defined potentials (E) to the working electrode relative to the reference electrode (commonly Ag/AgCl electrodes or saturated calomel electrodes, SCE). In addition to controlling E as an input variable, the potentiostat records the current (I) passing between the working electrode and the counter electrode. The currents are reductive or oxidative depending on whether electrons are transferred from or to the working electrode, respectively. The counter electrode closes the electrical circuit.

The current (units of ampere [A]) represents exchanged charge (Q) per time (t) (units of coulombs per second [C/s]). Accordingly, the measured current directly corresponds to the rate at which electrons are transferred across the working electrode surface at the applied E:

$$\text{rate of electron transfer} = \frac{dn_{e^-}}{dt} = \frac{I}{F} \tag{1}$$

where F is the Faraday constant (96485 [C/mol]) and n_{e^-} [mol] is the number of electrons transferred, which is obtained by integration of eq 1 over time:

$$\text{number of electrons transferred} = n_{e^-} = \int \frac{I}{F} dt \tag{2}$$

Depending on the experiment, the measured current may need to be corrected for the background current measured in the absence of the geochemical sample. Background currents arise from capacitive charging of the WE-solution interface as well as from slow electron transfer to and from species in solution

(e.g., slow reduction of protons at the WE surface at low applied potentials).

In amperometric techniques, the applied E may either be held constant over time (i.e., *constant potential techniques*) or varied systematically with time (i.e., *potentiodynamic techniques*). The most commonly used constant potential amperometric technique is chronoamperometry (origin: *chrono*, meaning time, *amperometry*, meaning measured current). There are a number of *potentiodynamic amperometric techniques*. Most commonly, the E is swept at a linear rate in so-called "potential sweep" techniques. The sweep may either be in only one potential direction (i.e., linear sweep voltammetry) or cycled between upper and lower vertex potentials (i.e., cyclic voltammetry). The data collected from these techniques is typically plotted as (cyclic) voltammograms, in which the measured I is plotted versus the applied E. The voltammograms provide insight into the E range over which electrons are transferred and the kinetics and reversibility of electron transfer to and from redox-active minerals (e.g., by examining current responses when sweeping in reductive and oxidative directions). The responses from potentiodynamic techniques are, however, often difficult to interpret (particularly in quantitative terms), especially if the working electrode and its surroundings are at disequilibrium with each other during measurements and/or if electron transfer is irreversible. In these cases, one must take caution when making thermodynamic arguments based on data from potentiodynamic measurements.

Potentiometric Techniques. Potentiometric measurements determine the reduction potentials of a sample relative to defined reference states. These potentials are also referred to as "open circuit potentials" (i.e., E^{OCP}), denoting that a high resistance is placed in the measurement circuit that impedes the exchange of electrons between the working electrode and the redox-active phase(s) during the measurements.[67,71] At the E^{OCP}, the rates of oxidation and reduction reactions at the working electrode surface are kinetically balanced, resulting in negligible net current flows. As a consequence, potentiometric measurements do not require a counter electrode and are typically conducted with only a working electrode and a reference electrode. Both electrodes can be combined in a single enclosure. Such combined electrodes include standard "redox" electrodes (e.g., a Pt ring working electrode combined with an Ag/AgCl reference electrode), pH electrodes, as well as other electrodes commonly used in water quality measurements.

While OCP measurements are easy to conduct, the data obtained require cautious interpretation because the measured E^{OCP} values correspond to the E of the redox-active phase(s) *only* if redox equilibration is obtained between the working electrode and phase(s) during the measurement. However, redox equilibration is often (extremely) slow, resulting in small, yet continuous drifts of E^{OCP}. Furthermore, redox electrodes may become poisoned over time (e.g., the formation of hydroxides and sulfides on the electrode surface). In all of these cases, the systems are prone to measurement artifacts, in that the measured E^{OCP} values do not reflect the true E of the mineral(s), as detailed in the next section.

Challenges and Intrinsic Complexity of Electrochemical Analyses of Redox-Active Minerals. The largest challenge in using electrochemical techniques for the characterization of redox-active minerals is to *attain redox equilibrium* between the mineral sample and working electrode. Many

minerals show slow or nonexisting redox equilibration with electrodes and thus give rise to artifacts in both amperometric and potentiometric measurements. The lack of redox equilibria has been documented for several systems containing suspended redox-active minerals.[72−75] A further complication can arise when samples contain more than one redox-active species at different potentials that transfer electron to and from the working electrode at different rates. These systems may produce so-called "mixed potentials" that result from different phases contributing to the net measured potential.[76,77] The most common strategies to promote mineral−electrode redox equilibration are (i) to bring the mineral in direct contact with an underlying working electrode (or even using the mineral *as* the working electrode), as discussed in the section on nonmediated analyses, and (ii) to use dissolved redox mediators that rapidly equilibrate with both the working electrode and mineral sample, as detailed in the section on mediated analyses.

Even if equilibrium is attained, the electrochemical analyses of minerals remain challenging, as a number of intrinsic mineral properties affect electrochemical responses, including mineral purity, crystallinity, and electronic structure as well as the chemistry, morphology, and size distribution of mineral particles.[61,78] The dependence of electrochemical responses on mineral purity and composition can be used to discriminate between solid solutions (i.e., a single mineral phase containing elemental impurities) and mechanical mixtures of two or more distinct mineral phases.[61] The crystallinity of a mineral may change as a direct result of electron transfer to and from the mineral in amperometric analyses. For instance, electron transfer to ferrihydrite can facilitate a secondary mineral transformation into thermodynamically more stable iron oxides, such as lepidocrocite.[79] Smaller particles typically exhibit faster electron transfer rates than larger particulate samples,[75] consistent with the increase in specific surface areas with decreasing particle sizes.[80] Consequently, mineral samples with wide particle size distributions exhibit complex electron transfer kinetics.[80−82] Mineral particle sizes and morphologies—and hence, the current responses—may change during amperometric analyses of minerals that undergo partial or complete dissolution during reduction or oxidation, as observed for iron and manganese oxides (e.g., Fe^{2+} is soluble at neutral pH values, while Fe^{3+} is insoluble).[80,81,83] Mineral dissolution may further compromise measurements if the dissolved metals subsequently reprecipitate as a new phase at the mineral-electrode interface. This phenomenon has been reported for cyclic voltammetry experiments with alternating reducing and oxidizing conditions.[84,85]

Multiple approaches have been developed to attain redox equilibration between minerals and working electrodes, which are reviewed in the next two sections, covering nonmediated and mediated analyses, respectively. The former summarizes work that relied on bringing the minerals into direct contact with the working electrode surface to facilitate equilibrium. The latter presents strategies that use dissolved redox mediators to facilitate redox equilibration and highlights some of the unique analytical insights into mineral redox properties that this approach provides.

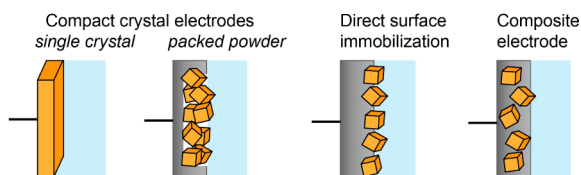## ■ NONMEDIATED ELECTROCHEMICAL ANALYSES OF REDOX-ACTIVE MINERALS

To establish redox equilibrium between a redox-active mineral and a solution over the course of electrochemical measure-
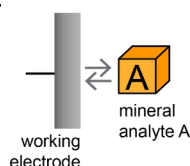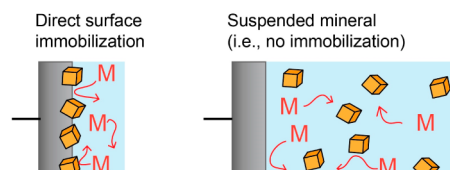
Figure 1. Overview of approaches to establish redox equilibration between the mineral analyte (A) and the working electrode (gray bar) in nonmediated (top) and mediated (bottom) electrochemical analyses of mineral analytes. In mediated electrochemical analyses, water-soluble redox mediators (M) are added to facilitate redox equilibration between the working electrode and A.

ments, past studies have most commonly relied on placing the mineral in direct physical contact with an existing working electrode surface or embedding the mineral into a conductive matrix that covers an underlying existing working electrode; in both cases, the mineral phase subsequently served as the working electrode (Figure 1). We refer to these approaches collectively as "non-mediated", to denote that no soluble redox mediators are added to facilitate electron transfer between the electrode and the mineral. The three most common approaches are to directly use the mineral as the working electrode (i.e., *compact crystal electrodes*), to impregnate the surface of an inert working electrode with mineral particles (i.e., *direct immobilization*), and to mix the mineral into a conductive matrix that serves as the working electrode (i.e., *composite electrodes*) (Figure 1). The following subsections summarize results of past studies that have used these three approaches. The summary is concise in recognition of several more extensive reviews on these approaches.[61,62,70,86] In contrast to past reviews, we highlight the major challenges in interpreting data collected with these approaches. In this review, we omit film-based electrodes, including clay-modified electrodes, given that these electrodes are commonly used to study the interactions of the mineral film with dissolved electroactive species and not necessarily the redox properties of the minerals that constitute the films.[87]

Compact Crystal Electrodes. The simplest means to establish redox equilibrium with a mineral in nonmediated electrochemical measurements is to have the mineral specimen become the working electrode (i.e., *compact crystal electrode*). This approach differs from the others in that the constructed electrode contains no additives, such as conductive binders. These electrodes are generally made using two strategies. In the first, a large natural or fabricated single mineral crystal with dimensions on the mm to cm scale is used as the working electrode. This approach allows one to probe reactions at specific crystal faces of the mineral, which are exposed to the solution.[28,88,89] The second strategy is to create a compacted powder-based electrode (often referred to as *packed powder disk electrodes*). This approach allows analyzing minerals for which large single crystals are not available. Here, a mineral powder is

packed into a cavity between an existing working electrode surface and the aqueous solution. The packing may involve high pressure and/or sintering at elevated temperatures. However, these treatments can lead to unwanted mineral transformations.[61] Packed powder disk electrodes can be used to study the effects of mineral particle size on reactivity.[90,91]

Compact crystal electrodes have been used to investigate basic redox properties and transformation processes of (semi)conducting minerals. Most commonly, the reductive or oxidative dissolution behavior of a mineral under a constant applied potential is assessed to elucidate corrosion mechanisms and rates.[63,84,92−98] These electrodes are also used to potentiometrically measure the E^{OCP} values of the minerals under defined solution conditions.[58,63,95,97,99,100] This approach is particularly useful in analyzing specimens that lack thermodynamic reference values, such as nanoparticles.[58,95,100] The electrodes may also be used in potentiodynamic amperometric measurements to determine the E values at which the minerals undergo reduction and oxidation reactions.[84,90,91,93,94,99,101−103] The obtained data sets allow relating observed reaction rates to applied potentials, as shown by Nurmi et al. for several fabricated Fe^0 nanoparticles.[101] Compact crystal electrodes require conduction in the mineral, thus excluding non- or poorly conducting minerals (such as goethite or iron-bearing clay minerals) from this analysis.

Direct Mineral Immobilization. In the second approach, *direct immobilization*, a mineral is impregnated into the surface of a soft host electrode that is relatively inert with respect to the solution, such as graphite, pencil lead, or gold. The embedding process typically involves pressing or grinding the working electrode against the mineral, which may be a macroscopic solid or a powder.[61] The embedded material may be used as is or heated to create a thin (μm-scale) homogeneous film.[102,104] The main advantages of this technique are that the electrodes are easy to prepare relative to other nonmediated electrochemical techniques and require only small amounts of the mineral (typically on the order of micrograms).

Similar to compact crystal electrodes, this approach is commonly used in amperometric measurements to assess reductive and oxidative mineral dissolution. Among these

techniques is abrasive stripping voltammetry, in which abrasion and stripping refer to the immobilization process and subsequent mineral dissolution, respectively.[105] This approach has been successfully applied to characterize the reductive dissolution of several iron (oxyhydr-)oxides as a function of electron transfer rates into the oxide,[106] solution chemistry and mineral particle shape and morphology.[107,108]

Composite Electrodes. In the third and final approach, *composite electrodes* are prepared by mixing the mineral with a conductive additive, and, in some cases, a binder material.[109,110] Composite electrodes are often formed using carbonaceous conductive additives (e.g., carbon black, acetylene black, milled graphite) and are then referred to as *carbon paste (electroactive) electrodes*.[61,110−113] This approach is particularly valuable for minerals that lack the intrinsic high conductivity required for compact crystal electrode measurements. However, the conductive additive may react with the embedded mineral or with products formed and thereby affect the electrochemical responses.[62,109,114] Furthermore, the construction of composite electrodes is relatively labor intensive and intricate. While composite electrodes are frequently used to study phases relevant to energy storage, there are relatively few studies on environmentally relevant iron- and manganese containing minerals.[109,114,115]

Major Challenges in Nonmediated Electrochemical Analyses. While nonmediated electrochemical analyses have advanced the general understanding of redox processes involving minerals, the approaches collectively face three major challenges. First, an inherent problem arises when using mineral phases that are nonconductive or semiconducting, as they can exhibit complex band bending phenomena when brought into direct contact with an existing metal working electrode.[116] This band bending can significantly alter both the measured potentials and the kinetics or electron transfer between the mineral phase of interest and the underlying working electrode. These effects are difficult and often practically impossible to account for when performing measurements. Second, different nonmediated electrochemical techniques applied to the same sample may yield conflicting results. For instance, the reductive dissolution of lead oxides assessed in composite electrodes and via direct immobilization resulted in different E values at which dissolution occurred and different reversibilities of electron transfer.[117] Another study showed that two procedures of preparing composite electrodes with ferrocene resulted in E values for the ferrocene/ferrocenium redox couple that differed by as much as 150 mV.[118] The third major drawback is that it is difficult, and in some cases impossible, to accurately control and/or quantify the amount of electrochemically active mineral that is transferred to the constructed electrodes, particularly when using packed bed electrodes or direct immobilization approaches. If the amount of added mineral remains poorly defined, it is impossible to quantify the fraction of the redox-active elements in the mineral that is electroactive in amperometric measurements. Previous work has found that this fraction can depend on several factors, including the particle size of the mineral, the presence of complexing agents in the binder of composite electrodes (e.g., oxalate),[114] the binder thickness, the type of potentiodynamic technique used, and experimental parameters used during measurements (e.g., the scan rate).[109] These issues imply that complementary techniques are needed to quantitatively relate E values to the redox state of an element in the mineral.[61]

■ MEDIATED ELECTROCHEMICAL ANALYSIS OF REDOX-ACTIVE MINERALS

Mediated electrochemical analyses offer an alternative, yet rarely utilized, means to assess the redox properties of minerals. In these analyses, dissolved redox-active compounds, called redox mediators (M), are added to the solution to facilitate electron transfer and E equilibration between the working electrode and mineral particles in the electrochemical cell (Figure 1). Typically, carbonaceous working electrodes are used that are chemically inert and have a wide potential window in aqueous solutions (e.g., vitreous or glassy carbon). Redox mediators can be used in both amperometric and potentiometric measurements.

Figure 2a,b shows the general principles of two complementary amperometric techniques: mediated electrochemical reduction (MER) and mediated electrochemical oxidation (MEO). In MER, oxidized mediator species (M_{ox}) are added to an aqueous solution in the electrochemical cell and are reduced at the working electrode to form reduced mediator species (M_{red}). The extent of reduction is determined by the potential applied to the working electrode and the apparent standard reduction potential of the mediator under the experimental conditions, $E_H^{0\prime}$ (where the subscript H denotes that values are referenced to the standard hydrogen electrode (SHE), the superscript 0 that equal activities of oxidized and reduced analyte species are present, and the superscript ′ denotes that the potentials are corrected for experimental conditions (e.g., solution pH and concentration of reacting species) that deviate from standard state conditions). Upon attainment of redox equilibrium between the mediator and the working electrode, and hence stable current readings, the mineral is added to the cell either as a powder or suspended in a small solution volume. Electron transfer from M_{red} to the oxidized minerals (A_{ox}, where A stands for the more generic term "analyte") reduces redox-active elements in the mineral (e.g., Fe^{3+}) and thereby regenerates M_{ox}. M_{ox} is subsequently rereduced at the working electrode to M_{red}, resulting in a reductive current response (I_{red}), which is measured by the potentiostat. Electron transfer mediation in MEO proceeds in an analogous manner: electrochemically generated M_{ox} oxidizes A_{red}, thereby forming A_{ox} and M_{red}. The newly generated M_{red} is reoxidized to M_{ox} at the working electrode resulting in an oxidative current response (I_{ox}). Figure 2c shows a schematic of diquat-mediated electrochemical reduction of mineral-associated Fe^{3+} and ABTS-mediated electrochemical oxidation of mineral-associated Fe^{2+}.

Mediated electrochemical analyses have only recently been added to the environmental scientists' and geochemists' toolkits. However, this approach has been used in other fields for decades. Mediated electrochemical analyses were developed in the 1970s to study redox properties and reactivities of redox-active centers in proteins,[119−122] including cytochrome c oxidase,[123,124] cytochrome c,[120,124,125] myoglobin,[120] ferredoxin,[125−127] and ferritin.[128,129] The use of water-soluble redox mediators provided fast electron transfer between the working electrode and the redox-active centers of the proteins and thereby eliminated kinetic artifacts that resulted from sluggish electron transfer in nonmediated measurements. Mediators were successfully employed in different electrochemical techniques, including thin layer cyclic voltammetry,[125] stepped potential microcoulometry,[129,130] and controlled potential electrolysis.[131]
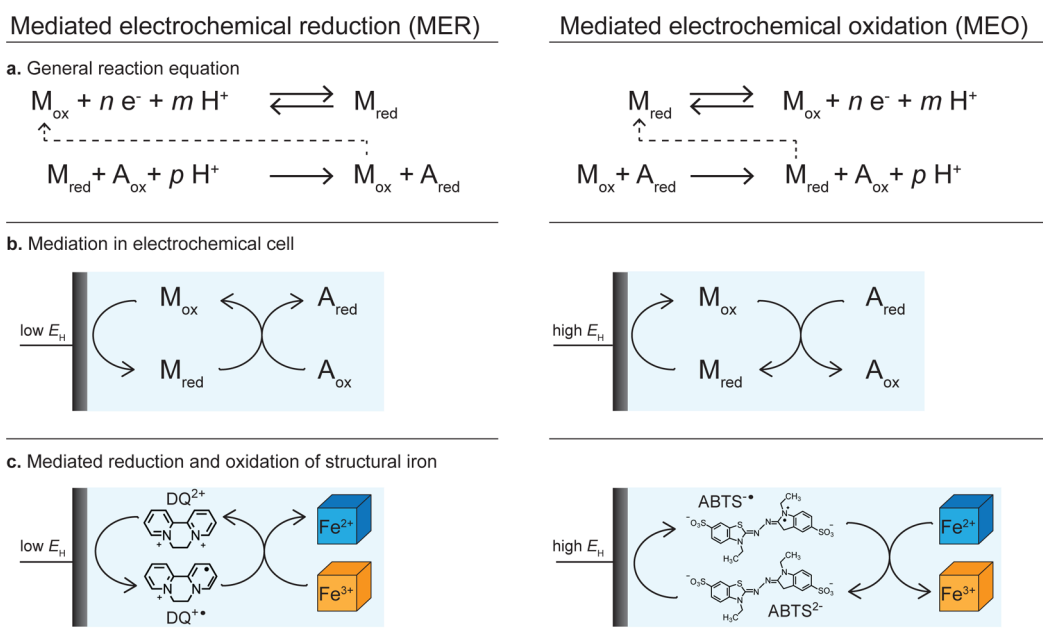
Figure 2. Schematic representation of mediated electrochemical reduction (MER) and mediated electrochemical oxidation (MEO). a. General reactions of MER and MEO involving mediator, M, mineral (which is abbreviated as A for "analyte"), electrons, e^-, and protons, H^+ (shown only for electrochemical reduction and oxidation of M with the respective stoichiometric reaction coefficients, n and m). The subscripts ox and red denote oxidized and reduced redox states. b. Depiction of MER and MEO in electrochemical cells with working electrodes polarized to low and high reduction potentials (E_H, V vs the standard hydrogen electrode, SHE), respectively. Electron transfer between the mediator (M) and the mineral specimen (A) occurs either at the working electrode−solution interface for immobilized minerals or in solution for suspended minerals. c. Examples of MER and MEO. In MER, the redox mediator—in this case diquat (DQ) − is reduced from its oxidized form (DQ^{2+}) to its reduced, radical form ($DQ^{+\bullet}$) at the working electrode. The $DQ^{+\bullet}$ then transfers an electron to the mineral containing structural ferric iron (Fe^{3+}), producing ferrous iron (Fe^{2+}) and DQ^{2+}. The DQ^{2+} is then rereduced at the working electrode that is polarized at a constant E_H. In MEO, the mediator ABTS is oxidized at the working electrode from its reduced state ($ABTS^{2-}$) to its one-electron oxidized state ($ABTS^{-\bullet}$). The $ABTS^{-\bullet}$ then accepts an electron from Fe^{2+}, forming $ABTS^{2-}$ and Fe^{3+}. $ABTS^{2-}$ is then reoxidized at the working electrode.

It is noteworthy that the use of redox mediators to facilitate electron transfer to minerals occurs naturally in the environment. Many dissimilatory metal reducing bacteria, including *Shewanella*[132−134] and *Geothrix*,[135] excrete endogenous and/or use exogenous extracellular "electron shuttling" compounds to transfer electrons to solid mineral substrates, including iron (oxyhydr-)oxides and particulate organic matter, during anaerobic respiration. A range of endogenous mediator compounds have been described,[136] among which flavins are considered the most important.[133,134,137,138] Flavins can be reduced in the extracellular space by cytochrome proteins on the outer membrane of the bacteria. The reduced flavins diffuse away from the bacterial cell toward the mineral surface, where they transfer electrons to solid-phase Fe^{3+}, forming Fe^{2+}. Reoxidized flavins that reach the bacterial cell close the catalytic cycle. The exogenous "electron shuttles" include dissolved organic matter present in soil and sediment pore waters.[139−141]

Only a few studies have applied mediated electrochemical analyses to minerals. In early work, this approach was successfully used to quantify the amount of redox-active iron on the surface of asbestos fibers.[142] Mediators were also used in potentiometric measurements of the E in natural sediments[143,144] and iron oxide suspensions.[145] However, in these studies, redox equilibration of the mediators with the sediment was not determined electrochemically, but instead monitored spectrophotometrically, making use of differences in the UV−vis absorbance spectra of the oxidized and the reduced mediator species. Recent work in our group and others[146] has demonstrated the unique possibilities of mediated electro-

chemical analyses to study the redox properties and reactivities of minerals and organic geochemical phases. We will highlight some of these possibilities below, following a discussion on the characteristics of suitable redox mediators. A detailed guide for setting up and conducting mediated amperometric and potentiometric analyses is provided in the Supporting Information.

Characteristics of Redox Mediators. To perform accurate and artifact-free mediated electrochemical analyses, one needs to carefully select appropriate mediator compounds that meet a number of important requirements[121] besides the most fundamental prerequisite of fast redox equilibration and electron transfer between the mediator and the analyte. The following subsection summarizes these requirements and provides a list of mediators that were successfully employed in recent redox analyses of structural iron in minerals[146−149] and redox-active functional groups in dissolved and particulate organic matter.[150−156]

Well-Defined Standard Reduction Potentials and Electron and Proton Transfer Stoichiometries. Redox mediators (M) must (i) undergo fully reversible electron transfer (i.e., both the reduced and oxidized mediator species should not undergo irreversible side reactions), (ii) have well-defined apparent standard reduction potentials under the experimental conditions, $E_H^{0'}$, and (iii) react with known reaction stoichiometries with respect to the numbers of electrons (n) and protons (m) transferred during reduction/oxidation (eq 3).

$$M_{ox} + n_{e^-} + m_{H^+} \rightleftharpoons M_{red} \tag{3}$$

Redox mediator	Oxidized species	Reduced species	$E_H^{0'}$ [V]	n e$^-$	m H$^+$
2,2'-Azino-bis(3-ethylbenzothiazoline-6-sulfonic acid) (ABTS$^{-\bullet}$ / ABTS^{2-})			+ 0.70	1	0
Ferrocene monocarboxylic acid			+ 0.51	1	0
Ferri/ferro-cyanide $[Fe(CN)_6]^{3-}$ / $[Fe(CN)_6]^{4-}$			+ 0.43	1	0
2,6-Dichlorophenol-indophenol			+ 0.25	2	2
Hexaammineruthenium			+ 0.09	1	0
1,4-Napthoquinone			+ 0.09	2	2
Resorufin (7-Hydroxy-3H-phenoxazin-3-one)			- 0.03	2	2
Cyanomethylviologen (1,1'-bis(cyanomethyl)-4,4'-bipyridyl)			- 0.14	1	0
Riboflavin 5'-monophosphate			- 0.18	2	2
Diquat (1,1'-ethylene-2,2'-bipyridyl) (DQ^{2+}/DQ$^{\bullet+}$)			- 0.35	1	0
4,4'-Bipyridinium-1,1'-bis(2-ethylsulfonate))			- 0.41	1	0
Ethylviologen (1,1'-bis(ethyl)-4,4'-bipyridyl)			- 0.45	1	0
Triquat (1,1'-trimethylene-2,2'-bipyridyl)			- 0.54	1	0

Figure 3. Redox mediators that have been used in mediated electrochemical analyses of particulate minerals and organic geochemical phases. The apparent standard reduction potential, $E_H^{0'}$, and the number of electrons, n, and protons, m, transferred to/from the mediators are given for pH 7. The $E_H^{0'}$ values are based on cyclic voltammetry measurements at pH 7.5,[148,149] corrected by +59 mV/pH for mediators with n = 2 and m = 2.

The use of mediators that undergo single electron transfers (i.e., n = 1) and are proton decoupled (i.e., m = 0) is preferable because they provide two unique features. First, single electron transfer mediators often exhibit much faster electron transfer rates than mediators of comparable $E_H^{0'}$ values that undergo proton coupled transfers of multiple electrons. Fast electron transfer is a key requirement to rapidly reach redox equilibrium conditions during measurements. Second, solution pH does not affect the speciation of M_{ox} and M_{red}. By comparison, mediators with coupled proton to electron transfers show pH-dependent protonation states of M_{ox} and/or M_{red} and, as a consequence, pH-dependent reactivities that can largely complicate data interpretation. For example, the two-electron reduction of a 1,4-quinone to a 1,4-hydroquinone is coupled to the transfer of two protons at acidic to circumneutral pH, one proton at slightly alkaline pH (to form the monophenolate species), and no proton at high pH (to form the diphenolate species). These different species may have different electron transfer rates with

minerals and the working electrode and may therefore bias mediated electrochemical analyses.[157]

Solubility and Stability in Aqueous Solutions over the Experimental pH Range. For reliable use of the mediators in aqueous systems, the oxidized and reduced mediator species must be soluble in water. Aqueous solubilities are high for charged (i.e., cationic, anionic, or zwitterionic) and some polar (i.e., H-bond accepting and donating) mediators, but not for nonpolar mediators. A second requirement is that the mediators must not degrade in water over the course of the electrochemical analyses. Control experiments are warranted for some mediators to assess their pH-dependent susceptibility to hydrolysis. Finally, the reduced and oxidized mediator species should not reduce protons (i.e., $H^+ + e^- \rightarrow \frac{1}{2} H_2$) nor oxidize water (i.e., $H_2O \rightarrow \frac{1}{2} O_2 + 2H^+ + 2e^-$) over the experimental pH range, respectively. This implies that the $E_H^{0'}$ of the mediator should lie inside the Pourbaix diagram (i.e., the E_H-pH stability diagram) of water. Previous studies have employed single redox mediators in electrochemical analyses. If
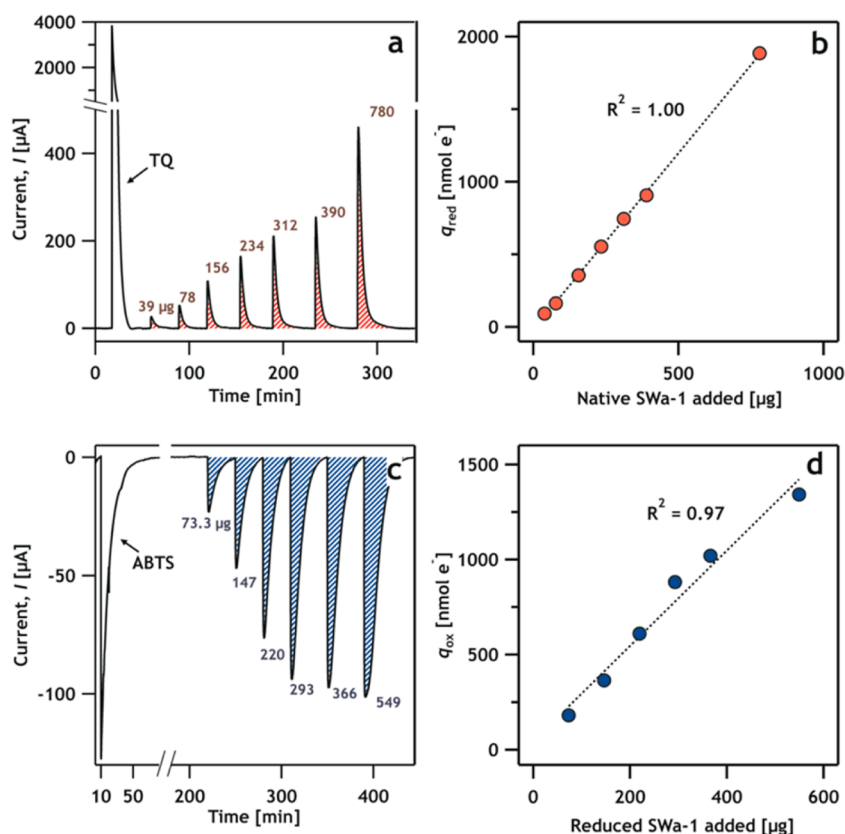
Figure 4. Current responses obtained from the triquat (TQ) mediated electrochemical reduction of structural Fe^{3+} in native smectite SWa-1 (panel a) and ABTS mediated electrochemical oxidation of structural Fe^{2+} in dithionite prereduced SWa-1 (panel c). The current peaks resulted from the addition of increasing amounts of suspended SWa-1, as indicated by the peak labels (in μg of SWa-1 added). In panels b and d, the total numbers of electrons transferred, q, are related to the mass of SWa-1 analyzed. Mediated electrochemical reduction and oxidation were conducted at applied potentials of $E_H = -0.60$ V and $+0.61$ V (vs. the standard hydrogen electrode) in pH 7.5 buffer solution. Reprinted (adapted) with permission from Gorski et al. *Environ. Sci. Technol.* 2012, 46 (17), 9360−9368. Copyright 2012 American Chemical Society.

mixtures of redox mediators are used to facilitate electron transfer over a wider E_H range, it is critical to first establish that the different mediators react with each other exclusively by electron transfer.[54]

Reversible Interactions of the Mediator with the Mineral and the Working Electrode. The mediator must get in close contact with both the mineral and the working electrode surfaces to allow for electron transfers. At the same time, strong and irreversible adsorption of the mediator to either of the two surfaces is undesirable because adsorption would lower the effective mediator concentration in solution and thereby decrease the rate of electron transfer. Furthermore, preferential adsorption of the oxidized or reduced mediator species is problematic because it would change the potential of the bulk solution as well as of the mineral surface. The resulting nonequilibrium between the solution and the E applied to the working electrode would result in an unwanted current response that is not due to electron transfer to/from the mineral but rather to mediator adsorption to the mineral. The same type of artifacts can result if the mediator forms complexes with mineral surfaces.

Several studies have assessed redox mediators for a range of applications.[54,143,158−167] The redox mediators that have been successfully employed to date in mediated electrochemical analyses of purified geochemical phases, including natural organic matter,[150−153,155,156,168−171] iron-bearing minerals,[147−149] iron (oxyhydr-)oxides,[146,172] and natural sediment

samples[172] are listed in Figure 3. The figure also lists the apparent standard reduction potentials of the mediators at pH 7 $(E_H^{0'})$, and the moles of electrons, n, and protons, m, that are transferred to/from one mole of each mediator. It is important to note that each depicted compound effectively mediates electron transfer only over a relatively narrow E_H range of approximately $E_H^{0'} \pm 120$ mV, according to the Nernst Equation. As a consequence, a large set of redox mediators is required to cover the entire range of environmentally relevant E_H values found in aqueous systems (i.e., from approximately $E_H = +0.8$ V to -0.5 V at circumneutral pH). Derivatives of 4,4′- and 2,2′-bipyridyls define a larger set of one electron transfer mediators that cover a wide $E_H^{0'}$ range and therefore can be used as mediators under reducing conditions. A commonly used mediator under oxidative conditions is ABTS due to its high first electron oxidation potential $(E_H^{0'} = 0.70$ V vs. SHE). We recently demonstrated that $ABTS^{\bullet-}/ABTS^{2-}$ can be also employed to quantify the antioxidant capacities of natural organic matter[151,168] and the concentrations of reduced structural iron in clay minerals.[147−149]

Information Obtained from Mediated Amperometric Analysis of Minerals. The current responses in mediated amperometric analyses of minerals allow determining (i) the number of electrons that are transferred to and from the analyte in MER and MEO, respectively, by integration of the current responses; (ii) the dependencies of electron transfer to and from the mineral on the E applied to the working electrode and

Table 1. Electron Accepting Capacity, EAC, at pH 7.5 and Applied Potential $E_H = -0.60$ V; Electron Donating Capacity, EDC, at pH 7.5 and $E_H = +0.61$ V, and Total Electron Exchanging Capacity, EEC (=EAC + EDC) of Several Specimens of the Ferruginous Smectite SWa-1[a]

sample pretreatment	EAC [mmol e-/g$_{SWa-1}$]	EDC [mmol e-/g$_{SWa-1}$]	EEC (=EAC + EDC) [mmol e-/g$_{SWa-1}$]	reduction index (RI)	EAC/ [Fe$_{total}$] [%]	EDC/ [Fe$_{total}$] [%]	EEC/ [Fe$_{total}$] (=CE) [%]
native (= untreated)	2.21 ± 0.05	0.00 ± 0.00	2.21 ± 0.05	0.00	97.8 ± 2.3	0.0 ± 0.0	97.8 ± 2.3
fully reduced by excess dithionite	0.05 ± 0.00	2.24 ± 0.02	2.29 ± 0.02	0.98	2.3 ± 0.5	99.1 ± 1.1	101.4 ± 1.2
partially reduced by stoichiometric amounts of dithionite	1.46 ± 0.05	0.76 ± 0.01	2.22 ± 0.05	0.34	64.7 ± 3.2	33.9 ± 1.5	98.6 ± 3.5
O$_2$ reoxidized of fully reduced	1.71 ± 0.02	0.44 ± 0.02	2.15 ± 0.03	0.20	76.0 ± 1.0	19.3 ± 5.1	95.3 ± 5.2

[a]The reduction index RI is defined RI = (EEC − EAC)/EEC = EDC/EEC. The capacities are related to the total structural Fe content ([Fe$_{total}$]) of SWa-1 (i.e., 12.6 wt % Fe) (CE = coulometric efficiency). Reprinted (adapted) with permission from Gorski et al. *Environ. Sci. Technol.*, 2012, *46* (17), 9360−9368. Copyright 2012 American Chemical Society.

on the solution pH, and (iii) the rates at which the electrons are transferred over the course of the mineral reduction or oxidation. The following two subsections address the first two points and, for illustrative purposes, include data obtained from mediated amperometric analyses of a well-characterized iron-bearing clay mineral (i.e., ferruginous smectite SWa-1).[147−149] The use of mediated amperometric analyses to study electron transfer rates to and from minerals has, so far, been explored to a lesser extent[146] and will thus be only briefly described. We do not discuss the results of potentiometric measurements because the obtained E_H^{OCP} values are straightforward to interpret, provided that redox equilibrium is attained.

Quantifying of the Number of Electrons Transferred to and from Minerals. The number of electrons transferred to and from a mineral, q_{red} and q_{ox} (both in moles of electrons, e$^−$), are quantified by integrating the reductive and oxidative current peaks obtained in MER and MEO, respectively (analogous to eq 2):

$$q_{red} = \frac{1}{F} \int_{t_0}^{t_{end}} (I_{red} - I_{red\ background}) dt \tag{4a}$$

$$q_{ox} = \frac{1}{F} \int_{t_0}^{t_{end}} (I_{ox} - I_{ox\ background}) dt \tag{4b}$$

where t_0 and t_{end} [s] define the integration boundaries of the current peaks, I_{red} and I_{ox} (both in units of amperes, [A] = [C/s]) correspond to the measured reductive and oxidative currents, and the subscript "background" stands for the respective background currents in the absence of the analyte.

Figure 4 shows an example for background-corrected reductive and oxidative current peaks in MER and MEO obtained by adding increasing amounts of the iron-bearing smectite SWa-1 (12.6 wt % Fe) to the electrochemical cells. MER was performed with triquat (TQ; Figure 3) on native SWa-1, in which all structural Fe was initially present as Fe^{3+}. MEO was performed with ABTS on dithionite pre-reduced SWa-1, in which 98% of the structural iron was initially present as Fe^{2+}. Figure 4b,d shows that q_{red} and q_{ox} increased linearly with increasing added amounts of the respective SWa-1 and therefore that the number of electrons transferred were directly proportional to the amount of added structural Fe^{3+} or Fe^{2+}. Figure 4 further illustrates the very low limits of quantification obtained by mediated amperometric analyses: electron transfer to as little as 88 nmoles of Fe^{3+} in 39 μg of SWa-1 was accurately quantified. This finding is particularly remarkable considering that the added iron was embedded in the silicate

mineral matrix and hence not freely dissolved in the electrochemical cell during analysis. We note that the addition of the same clay specimen to the electrochemical cells containing no mediators did not result in defined current responses.[147]

Determination of Electron Accepting and Donating Capacities of a Mineral. The numbers of electrons transferred to and from minerals in MER and MEO (i.e., q_{red} and q_{ox}) are expected to linearly correlate with the masses of added mineral, as shown exemplarily for SWa-1 in Figure 4b,d. The mass-normalized numbers of electrons transferred to and from a mineral are the so-called *electron accepting* and *donating capacities*, EAC and EDC (both [mol e$^−$/g$_A$]), respectively:

$$EAC = \frac{q_{red}}{m_A} \tag{5a}$$

$$EDC = \frac{q_{ox}}{m_A} \tag{5b}$$

where m_A [g] is the mass of the added mineral analyte. The sum of EAC and EDC, which we define as electron exchanging capacity EEC, is a direct measure of the total number of electrons that are transferred to and from the mineral analyte at the applied E values. For the later discussion, it is important to bear in mind that the EAC and EDC values (and hence also the EEC values) depend on the electrochemical conditions (i.e., reductive and oxidative E values applied to the working electrodes and the solution pH) used during mediated electrochemical reduction and oxidation, respectively.

In combination, the quantification of EAC and EDC values at very low and high applied potentials allows comparing the redox states of different minerals and, more importantly, determining changes in the redox state of a given mineral over the course of a reaction. For instance, at applied potentials of −0.60 V and +0.61 V, native SWa-1 containing only structural Fe^{3+} but no Fe^{2+} was found to have an EAC of 2.21 ± 0.01 mmol e−/g (Figure 4b, reflecting electron transfer to structural Fe^{3+} to form structural Fe^{2+}) and an EDC of 0 mmol e−/g (not shown; the absence of an oxidative current response is consistent with the lack of structural Fe^{2+} in native SWa-1 that could donate electrons to ABTS$^{−•}$). Dithionite reduction of the Fe^{3+} in native SWa-1 lowered the EAC to 0.05 ± 0.01 mmol e$^−$/g (not shown) while it increased the EDC to 2.24 ± 0.02 mmol e$^−$/g (Figure 4d). Intermediate EAC and EDC values were quantified for the native SWa-1 following partial reduction with dithionite and for the dithionite-reduced SWa-1
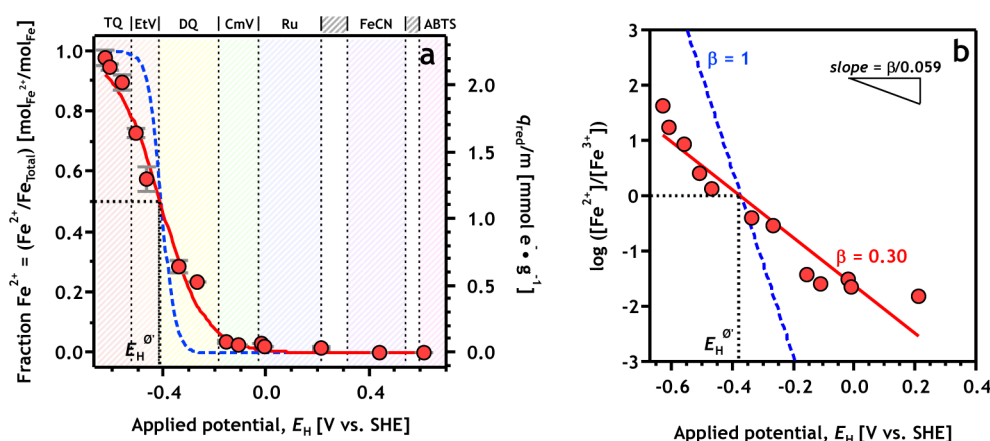
J

Figure 5. a. Fraction of total structural iron in SWa-1 smectite converted from Fe^{3+} to Fe^{2+} during mediated electrochemical reduction of native SWa-1 (i.e., all Fe^{3+}) as a function of the applied potential E_H. Different redox mediators were used at different potential ranges as indicated at the top of the Figure and the vertical dashed lines and included ABTS, hexacyanoferrate (FeCN), ruthenium hexamine (Ru), cyanomethyl viologen (CmV), diquat (DQ), ethyl viologen (EtV) and triquat (TQ) (from high to low E_H). All analyses were performed in pH 7.5 solution. b. The data from panel a replotted as the log concentration ratio of structural Fe^{2+} to Fe^{3+} versus E_H. The red symbols and lines represent experimental data and model fits. The dashed blue line corresponds to a hypothetical analyte with an ideal Nernst redox behavior ($\beta = 1$) and the same apparent standard reduction potential, $E_H^{\varnothing\prime}$, as SWa-1. Reprinted (adapted) with permission from Gorski et al., *Environ. Sci. Technol.* 2012, 46 (17), 9369−9377. Copyright 2012 American Chemical Society.

following partial reoxidation (Table 1). All specimens had very similar EEC values, indicating that no structural Fe was lost from this clay during the different sample treatments. Systems in which EEC values decrease or increase during redox cycling would instead reveal that redox-active constituents are lost from or formed in the mineral during sample treatment, respectively.

The extents of reduction of the different clay specimens can be quantitatively described by the Reduction Index, *RI*:

$$RI = \frac{EEC - EAC}{EEC} = \frac{EDC}{EEC} \quad (6)$$

The RI varies between 0 and 1 for fully reduced and oxidized specimens, respectively. Table 1 shows that the different treatments resulted in SWa-1 specimens with RI between 0.00 and 0.98. Clearly, these electrochemical analyses of redox states are much more easily carried out and sensitive than previous approaches that quantified Fe^{2+} and Fe^{3+} that were extracted from the clays through tedious and dangerous mineral dissolution using hydrofluoric acid.[173,174] The mediated electrochemical quantification of RI of a mineral can be complemented with spectroscopic analyses of the Fe redox states in the mineral using Mössbauer spectroscopy.

Determination of the Fraction of Redox-Active Elements in the Mineral That Participate in Electron Transfer. For well-characterized minerals with known concentrations of redox-active elements, it is possible to determine the fraction of the total redox-active elements that accept and donate electrons under the applied *E* and solution conditions (pH and ionic strength) employed in the mediated electrochemical analyses. We refer to this fraction as the *coulometric efficiency* (CE):

$$CE = \frac{EEC}{\sum_i a_i \cdot n_i} \quad (7)$$

where a_i, [mol a_i/g_A] is the molar concentration of the redox active element i in the analyte A; and n_i [mol e-/mol a_i] are the moles of electrons transferred to and from one mole of a_i.

Data collected with SWa-1 again serves as an illustrative example (Figure 4 and Table 1). The structural Fe content of SWa-1 was determined as $a_{total} = 2.26 \pm 0.02$ [mmol Fe/g]

following its complete digestion in acid.[147] For the Fe^{3+}/Fe^{2+} redox couple, n_i is 1 mol e$^-$/mol Fe. The calculated CE values of four SWa-1 specimen with different sample pretreatments ranged from 95.3 (±5.2) % to 101.4 (±1.2) %. These values imply that all structural Fe in SWa-1 was redox-active under the chosen electrochemical conditions and that the different sample treatments selectively altered the redox state of the structural Fe. We note that CE values much smaller than 100% were determined for other iron-bearing clay minerals under the same electrochemical conditions.[149] Mediated electrochemical analyses can therefore be used to assess how the microenvironments of redox-active elements in minerals govern bulk mineral redox properties including the fractions of the redox-active elements that readily undergo electron transfer with solution-phase redox mediators.

Determination of E and pH Dependence of Electron Transfer to/from the Mineral. As detailed in the previous discussion, all structural Fe in SWa-1 was electroactive when running MER and MEO at pH 7.5 and at very low and high applied potentials, respectively. Mediated electrochemical analyses may, however, also be used to quantify EAC and EDC values at intermediate applied E_H and as a function of the solution pH in the electrochemical cell. Systematic variations in E_H and pH can thus provide insights into the distribution of reduction potentials of the redox-active elements in the mineral and into the proton coupling of the electron transfers.

First, let us consider the mediated electrochemical analysis of a given mineral at different E_H values in MER and MEO while the solution pH is kept constant. For minerals with known concentrations and initial redox states of the redox-active element a_i, the transferred number of electrons at intermediate applied E_H can be used to determine the concentrations of the reduced and oxidized species of a_i (i.e., $[a_{i,red}]$ and $[a_{i,ox}]$) as a function of applied E_H. As an illustrative example Figure 5 shows the results of MER experiments in which aliquots of fully oxidized, native SWa-1 (i.e., 100% Fe^{3+}) were added to cells poised to different E_H. In this figure, the numbers of electrons transferred to Fe^{3+} are expressed as the formed Fe^{2+} normalized to the total structural Fe in SWa-1, Fe_{total}. The resulting
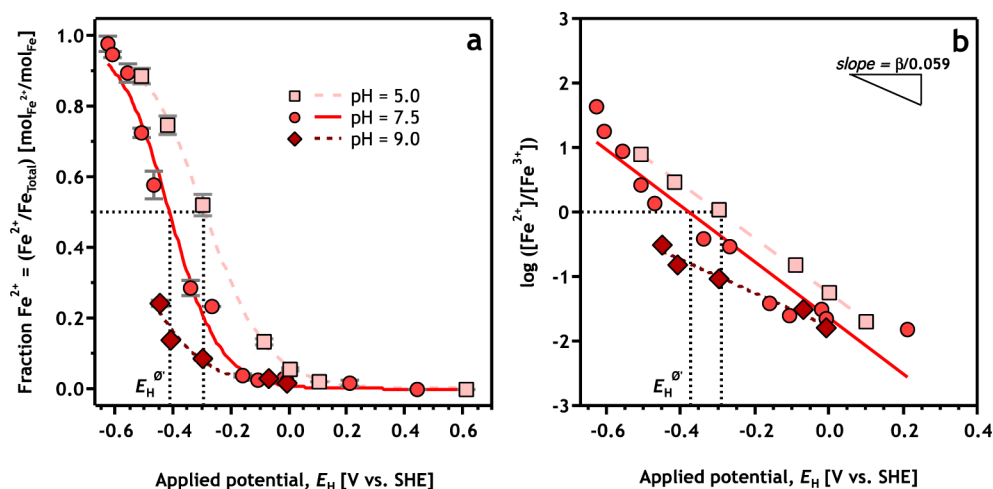
Figure 6. a. Fraction of total structural iron in SWa-1 smectite converted from Fe^{3+} to Fe^{2+} during mediated electrochemical reduction of native SWa-1 (i.e., all Fe^{3+}) as a function of the solution pH and the applied potential E_H. b. The data from panel a replotted as the log concentration ratio of structural Fe^{2+} to Fe^{3+} versus E_H. The symbols and lines represent experimental data and model fits, respectively. $E_H^{\emptyset'}$ corresponds to the apparent standard reduction potentials of the clay mineral. The pH 7.5 data in both panels is replotted from Figure 5a.

dependency of Fe^{2+}/Fe_{total} (i.e., of the reduction index, RI) on E_H has a sigmoidal shape and can be well described by a modified Nernst equation:[148]

$$E_H = E_H^{\phi'} - \frac{2.303 \cdot R \cdot T}{n_i \cdot F} \cdot \frac{1}{\beta} \cdot \log \frac{[a_{i,red}]}{[a_{i,ox}]} \quad (8)$$

where $E_H^{\emptyset'}$ [V] is the apparent standard reduction potential of the mineral under the used solution conditions, R [J/(mol K)] is the universal gas constant, T [K] is the absolute temperature, F is the Faraday constant [96485 C/mol], n_i [mol e^-/mol a_i] is the stoichiometry of electron transfer between the reduced and oxidized solid-state species, $a_{i,red}$ and $a_{i,ox}$, respectively (i.e., in the case of SWa-1, $a_{i,red}$ and $a_{i,ox}$ correspond to Fe^{2+} and Fe^{3+}, respectively, and $n_{Fe} = 1$ mol e^-/mol Fe). The dimensionless factor β ranges between 0 and 1 with decreasing values indicating widening of the E_H range over which electrons are accepted and donated relative to the ideal Nernst case (i.e., $\beta = 1$). $[a_{i,red}]$ and $[a_{i,ox}]$ denote the solid-state concentrations (as approximations of activities) of the reduced and the oxidized species of a_i. We deliberately report apparent standard reduction potentials ($E_H^{\emptyset'}$) instead of true standard reduction potentials ($E_H^{0'}$) to account for the fact that the dependency of the redox state of a mineral on the applied E_H may involve metastable states in the solid.[148]

Equation 8 can be rearranged to

$$\log \frac{[a_{i,red}]}{[a_{i,ox}]} = -\beta \cdot \frac{n_i \cdot F}{2.303 \cdot R \cdot T} \cdot (E_H - E_H^{\phi'}) \quad (9)$$

Plots of $\log([a_{i,red}]/[a_{i,ox}])$ versus the applied E_H can be fitted by a straight line with a slope of $-(\beta \cdot n_i)/0.059$ at $T = 20$ °C. The $E_H^{\emptyset'}$ corresponds to the E_H at which $[a_{i,red}] = [a_{i,ox}]$ and hence $\log([a_{i,red}]/[a_{i,ox}]) = 0$.

The data from Figure 5a is replotted in the linearized form in Figure 5b $\log([Fe^{2+}]/[Fe^{3+}])$ versus the E_H. The regression line yields an $E_H^{\emptyset'}$ of -0.41 (± 0.01) V and a β value of 0.30 (± 0.02). The low β value implies that electrons were transferred to Fe^{3+} in the SWa-1 over a much wider E_H range (i.e., 0.8 V) than expected if ideal Nernstian redox behavior had applied (i.e., $\beta = 1$ and 99% redox conversion of the analyte over a potential range of 0.24 V). This finding implies that

native SWa-1 may act as an electron acceptor over wide E_H ranges in natural systems. A more detailed discussion of the potential distribution of redox-active iron in SWa-1 and additional iron-bearing clay minerals as well as the reversibility of and electron transfer to and from structural iron are provided elsewhere.[147−149]

If the electron transfer to and from redox active elements a_i in the mineral is coupled to proton transfer, then the E_H of the mineral is expected to depend on the solution pH. Mediated electrochemical analyses offers the possibility to assess proton coupled electron transfer by varying the solution pH in the electrochemical cell. The independent control of pH and E_H is a unique advantage of the electrochemical approach over other techniques that rely on reacting the minerals with bulk chemical reductants and oxidants, many of which have pH dependent redox properties and reactivities. An example for mediated electrochemical analysis of minerals at different pH values is given in Figure 6 for native SWa-1. The extents of structural Fe^{3+} reduction in native SWa-1 for a constant applied E_H increased with decreasing pH from and pH 9 to 7.5 and 5. This pH dependence suggests that the reduction of structural Fe was coupled to proton consumption,[175,176] consistent with previous observations and calculations.[175,177−179] A similar setup of mediated electrochemical analyses may be used to determine the proton to electron transfer stoichiometries in the reductive dissolutions of Fe (oxyhydr-)oxides.

Determination of Rates of Electron Transfer to/from the Mineral. As previously discussed, the background-corrected current at any given time during the electrochemical analysis directly corresponds to the *rate* at which electrons are transferred across the working electrode surface.[67] In principle, this measured rate of electron transfer can be limited by one of three steps: (i) the electron transfer between the mediator and the mineral (which itself may be controlled by the rate of electron transfer in the mineral), (ii) the mass transfer of the mediator between the mineral and the working electrode, and (iii) the electron transfer between the mediator and the working electrode.

For systems in which the rate is limited by step (i), a second-order electron transfer rate can be estimated by the following relationship (as detailed in the Supporting Information):

$$-k_{\mathrm{ET}} \cdot [M_{\mathrm{red/ox}}] \cdot t = \ln\left(1 - \frac{\int_{t_0}^{t}\left(\frac{1}{F} \cdot I(t)\right)\mathrm{d}t}{\int_{t_0}^{t_\infty}\left(\frac{1}{F} \cdot I(t)\right)\mathrm{d}t}\right) \tag{10}$$

where k_{ET} [L mol^{-1} s^{-1}] is the second order rate constant, $[M_{\mathrm{red/ox}}]$ (units of [mol L^{-1}]) is the concentration of the reduced/oxidized mediator in MER/MEO, t is the time [s], t_0 [s] is the time at which the mineral is added to the electrochemical cell (i.e., onset of MER/MEO), t_∞ [s] is the time at which all electroactive elements have been reduced/oxidized in MER/MEO (i.e., time at which the current is back to background values), F is the Faraday constant [C/mol], and $I(t)$ [A] is the background-corrected reductive/oxidative current response in MER/MEO at time t. The second order rate constant k_{ET} can be obtained from the slope of a regression line of $\ln\left(1 - \left((\int_{t_0}^{t}((1/F) \cdot I(t))\mathrm{d}t)/(\int_{t_0}^{t_\infty}((1/F) \cdot I(t))\mathrm{d}t)\right)\right)$ versus t.

It is possible to assess whether step (i) or the steps (ii) and (iii) are rate determining for a given system by also analyzing the baseline-corrected current response resulting from the addition of a small amount of the mediator to the electrochemical cell, according to eq 10. Mineral-mediator combinations in which the rate of step (i) is comparable or faster than the combined rate of steps (ii) and (iii) cannot be kinetically interpreted using the above-described setup of constant potential amperometry. For such systems, the regression lines of $\ln\left(1 - \left((\int_{t_0}^{t}((1/F) \cdot I(t))\mathrm{d}t)/(\int_{t_0}^{t_\infty}((1/F) \cdot I(t))\mathrm{d}t)\right)\right)$ versus t for the analyses of analyte peaks will be comparable or identical to the slopes obtained from analyzing mediator peaks.

However, rate limitation by steps (ii) and (iii) can typically be eliminated by continuously stirring the solution in the electrochemical cell during the analysis and by choosing redox mediators that undergo rapid electron transfer with the working electrode, respectively. Systems in which step (i) is slower than the combined steps (ii) and (iii) will have smaller slopes of $\ln\left(1 - \left((\int_{t_0}^{t}((1/F) \cdot I(t))\mathrm{d}t)/(\int_{t_0}^{t_\infty}((1/F) \cdot I(t))\mathrm{d}t)\right)\right)$ versus t when analyzing the current peaks in responses to the addition of the minerals as compared to those obtained from adding the mediator. In these systems, the current response is a direct measure for the electron transfer between the mediator and the mineral. Using this approach, a systematic analysis of electron transfer rates as a function of the E and pH of a system as well as on the physicochemical properties of the electron transfer mediator is a promising means to link mineral redox reactivity to thermodynamics. We expect that this approach will be used to quantitatively describe differences in the reactivity of minerals and to link these differences to mineral crystallinity.

■ SUMMARY REMARKS AND OUTLOOK

This review highlights the distinct capabilities of analytical electrochemistry and, in particular, mediated electrochemical analyses in directly measuring the redox properties and reactivities of particulate mineral phases. We anticipate that mediated electrochemical analysis will become a frequently used technique for characterizing both mineral and solid organic geochemical phases. The obtained insights into the redox properties and reactivities of the minerals will largely advance our understanding of redox reactions involving geochemical phases and their effects on the cycling of elements and nutrients as well as on the fate and toxicity of organic and inorganic pollutants. We note that mediated electrochemical

analysis is also applicable to minerals that undergo reductive dissolution. In fact, the electrochemical approach offers unique advantages over batch studies to systematically study reductive mineral dissolution in that the rates of electron transfer to such minerals can easily be assessed as a function of E_{H} and solution pH.

In the near future, we foresee that mediated electrochemical analyses as an analytical technique will be advanced with respect to the following features. First, we expect that the list of suitable redox mediators will be further extended. New mediators may be synthesized to increase the coverage of the environmentally relevant range of reduction potentials. Sets of mediators with the same core structure but different substituents may be employed to assess how mediator interactions with the mineral surface affect electron transfer.[180] Second, future work will be directed toward miniaturizing the working electrodes used in the electrochemical analyses. Such miniaturizations will further lower the amounts of material needed for the analysis. The use of μm-sized working electrodes mounted in micromanipulation stages will open the possibility to map the spatial heterogeneity of mineral surface redox properties at μm resolution. In fact, some of these features are already implemented in scanning electrochemical microscopy (SECM), a surface analysis technique that relies on using dissolved redox-active mediators in solution to characterize surfaces.[181−183] We anticipate that SECM will become more intensely used in geochemical research over the next years. Third, future studies can combine mediated amperometric and potentiometric measurements with other techniques, such as spectroscopic analyses, to directly link electron transfer rates and thermodynamics to molecular-scale and bulk mineral properties.

Mediated electrochemical analysis is universally applicable to redox-active particulate samples. In addition to well-characterized mineral and organic geochemical phases, the analyzed samples may include poorly defined natural samples that contain mixtures of redox-active minerals and organic constituents. In these cases, mediated electrochemical analyses combined with spectroscopic and elemental composition analyses will open new possibilities to identify the predominant redox-active constituents in complex samples and to assess their relative importance to the overall redox properties of a bulk sample. Mediated electrochemical analyses can also be used in future studies to directly monitor changes in the redox states of geochemical phases during abiotic and biotic redox processes in an integrative manner. As such, mediated electrochemical analyses offers unprecedented analytical capabilities to close electron budgets and to assess the reversibility of electron transfer in redox reactions involving mineral and organic geochemical phases.

■ ASSOCIATED CONTENT

⑤ Supporting Information

Detailed description on the experimental setup for mediated amperometric and potentiometric measurements. A derivation of equation 10. This material is available free of charge via the Internet at http://pubs.acs.org.

■ AUTHOR INFORMATION

Corresponding Authors

*(M.S.) Phone: +41 (0)44 632-8314; fax: +41 (0)44 633-1122; e-mail: michael.sander@env.ethz.ch.

*(C.A.G.) Phone: +1 (814) 865-5673; fax: +1 (814) 863-7304; e-mail: gorski@engr.psu.edu.

Notes

The authors declare no competing financial interest.

■ REFERENCES

(1) Melton, E. D.; Swanner, E. D.; Behrens, S.; Schmidt, C.; Kappler, A. *The Interplay of Microbially Mediated and Abiotic Reactions in the Biogeochemical Fe Cycle*; Nature Publishing Group, 2014; pp 1−12.

(2) Brown, G. E.; Henrich, V. E.; Casey, W. H.; Clark, D. L.; Eggleston, C.; Felmy, A.; Goodman, D. W.; Gratzel, M.; Maciel, G.; McCarthy, M. I.; Nealson, K. H.; Sverjensky, D. A.; Toney, M. F.; Zachara, J. M. Metal oxide surfaces and their interactions with aqueous solutions and microbial organisms. *Chem. Rev.* **1999**, *99* (1), 77−174.

(3) Borch, T.; Campbell, K.; Kretzschmar, R. How electron flow controls contaminant dynamics. *Environ. Sci. Technol.* **2009**, *44* (1), 3−6.

(4) Borch, T.; Kretzschmar, R.; Kappler, A.; Van Cappellen, P.; Ginder-Vogel, M.; Voegelin, A.; Campbell, K. Biogeochemical redox processes and their impact on contaminant dynamics. *Environ. Sci. Technol.* **2010**, *44* (1), 15−23.

(5) Konhauser, K. O.; Kappler, A.; Roden, E. E. Iron in microbial metabolisms. *Elements* **2011**, *7* (2), 89−93.

(6) Johnson, C. M.; Beard, B. L. Biogeochemical cycling of iron isotopes. *Science (New York, N.Y.)* **2005**, *309*, 1025−1027.

(7) Rickard, D.; Luther, G. W. Chemistry of iron sulfides. *Chem. Rev.* **2007**, *107* (2), 514−562.

(8) Roden, E. E. Fe(III) oxide reactivity toward biological versus chemical reduction. *Environ. Sci. Technol.* **2003**, *37* (7), 1319−1324.

(9) Roden, E. E. Microbial iron-redox cycling in subsurface environments. *Biochem. Soc. Trans.* **2012**, *40*, 1249−1256.

(10) Roden, E. E.; Urrutia, M. M.; Mann, C. J. Bacterial reductive dissolution of crystalline Fe(III) oxide in continuous-flow column reactors. *Appl. Environ. Microbiol.* **2000**, *66* (3), 1062−1065.

(11) Benner, S. G.; Hansel, C. M.; Wielinga, B. W.; Barber, T. M.; Fendorf, S. Reductive dissolution and biomineralization of iron hydroxide under dynamic flow conditions. *Environ. Sci. Technol.* **2002**, *36* (8), 1705−1711.

(12) Cummings, D. E.; Caccavo, F.; Fendorf, S.; Rosenzweig, R. F. Arsenic mobilization by the dissimilatory Fe(III)-reducing bacterium Shewanella alga BrY. *Environ. Sci. Technol.* **1999**, *33* (5), 723−729.

(13) Hedges, J. I.; Keil, R. G. Sedimentary organic-matter preservation - An assessment and speculative synthesis. *Mar. Chem.* **1995**, *49* (2−3), 81−115.

(14) Kaiser, K.; Guggenberger, G. The role of DOM sorption to mineral surfaces in the preservation of organic matter in soils. *Org. Geochem.* **2000**, *31* (7−8), 711−725.

(15) Lalonde, K.; Mucci, A.; Ouellet, A.; Gelinas, Y. Preservation of organic matter in sediments promoted by iron. *Nature* **2012**, *483* (7388), 198−200.

(16) Riedel, T.; Zak, D.; Biester, H.; Dittmar, T. Iron traps terrestrially derived dissolved organic matter at redox interfaces. *Proc. Natl. Acad. Sci. U.S.A.* **2013**, *110* (25), 10101−10105.

(17) Klausen, J.; Trober, S. P.; Haderlein, S. B.; Schwarzenbach, R. P. Reduction of substituted nitrobenzenes by Fe(II) in aqueous mineral suspensions. *Environ. Sci. Technol.* **1995**, *29* (9), 2396−2404.

(18) Haderlein, S. B.; Pecher, K., Pollutant Reduction in Heterogeneous Fe(II)-Fe(III) Systems. In *Mineral-Water Interfacial Reactions*; Sparks, D. L., Grundl, T. J., Eds.; American Chemical Society, 1998; Vol. *715*, pp 342−357.

(19) Amstaetter, K.; Borch, T.; Larese-Casanova, P.; Kappler, A. Redox transformation of arsenic by Fe(II)-activated goethite (alpha-FeOOH). *Environ. Sci. Technol.* **2010**, *44* (1), 102−108.

(20) Charlet, L.; Scheinost, A. C.; Tournassat, C.; Greneche, J. M.; Gehin, A.; Fernandez-Martinez, A.; Coudert, S.; Tisserand, D.; Brendle, J. Electron transfer at the mineral/water interface: Selenium reduction by ferrous iron sorbed on clay. *Geochim. Cosmochim. Acta* **2007**, *71* (23), 5731−5749.

(21) Elsner, M.; Haderlein, S. B.; Kellerhals, T.; Luzi, S.; Zwank, L.; Angst, W.; Schwarzenbach, R. P. Mechanisms and products of surface-mediated reductive dehalogenation of carbon tetrachloride by Fe(II) on goethite. *Environ. Sci. Technol.* **2004**, *38* (7), 2058−2066.

(22) Klausen, J.; Haderlein, S. B.; Schwarzenbach, R. P. Oxidation of substituted anilines by aqueous MnO_2: Effect of co-solutes on initial and quasi-steady-state kinetics. *Environ. Sci. Technol.* **1997**, *31* (9), 2642−2649.

(23) Remucal, C. K.; Ginder-Vogel, M. A critical review of the reactivity of manganese oxides with organic contaminants. *Environ. Sci.: Processes Impacts* **2014**, *16* (6), 1247−1266.

(24) Strathmann, T. J.; Stone, A. T. Mineral surface catalysis of reactions between Fe(II) and oxime carbamate pesticides. *Geochim. Cosmochim. Acta* **2003**, *67* (15), 2775−2791.

(25) White, A. F.; Peterson, M. L. Reduction of aqueous transition metal species on the surfaces of Fe(II)-containing oxides. *Geochim. Cosmochim. Acta* **1996**, *60* (20), 3799−3814.

(26) Zhang, H. C.; Huang, C. H. Oxidative transformation of fluoroquinolone antibacterial agents and structurally related amines by manganese oxide. *Environ. Sci. Technol.* **2005**, *39* (12), 4474−4483.

(27) Rosso, K. M.; Yanina, S. V.; Gorski, C. A.; Larese-Casanova, P.; Scherer, M. M. Connecting observations of hematite (a-Fe_2O_3) growth catalyzed by Fe(II). *Environ. Sci. Technol.* **2010**, *44* (1), 61−67.

(28) Yanina, S. V.; Rosso, K. M. Linked reactivity at mineral-water interfaces through bulk crystal conduction. *Science* **2008**, *320* (5873), 218−222.

(29) Gorski, C. A.; Scherer, M. M., Fe^{2+} sorption at the Fe oxide-water interface: A revised conceptual framework. In *Aquatic Redox Chemistry*; Tratnyek, P. G., Grundl, T., Haderlein, S., Eds.; American Chemical Society, 2011; Vol. *1071*, pp 315−343.

(30) Pedersen, H. D.; Postma, D.; Jakobsen, R.; Larsen, O. Fast transformation of iron oxyhydroxides by the catalytic action of aqueous Fe(II). *Geochim. Cosmochim. Acta* **2005**, *69* (16), 3967−3977.

(31) Felmy, A. R.; Ilton, E. S.; Rosso, K. M.; Zachara, J. M. Interfacial reactivity of radionuclides: Emerging paradigms from molecular-level observations. *Mineral. Mag.* **2011**, *75* (4), 2379−2391.

(32) Gorski, C. A.; Handler, R. M.; Beard, B. L.; Pasakarnis, T.; Johnson, C. M.; Scherer, M. M. Fe atom exchange between aqueous Fe^{2+} and magnetite. *Environ. Sci. Technol.* **2012**, *46* (22), 12399−12407.

(33) Handler, R. M.; Beard, B. L.; Johnson, C. M.; Scherer, M. M. Atom Exchange between Aqueous Fe(II) and Goethite: An Fe Isotope Tracer Study. *Environ. Sci. Technol.* **2009**, *43* (4), 1102−1107.

(34) Hansel, C. M.; Benner, S. G.; Fendorf, S. Competing Fe(II)-induced mineralization pathways of ferrihydrite. *Environ. Sci. Technol.* **2005**, *39* (18), 7147−7153.

(35) Hansel, C. M.; Benner, S. G.; Neiss, J.; Dohnalkova, A.; Kukkadapu, R. K.; Fendorf, S. Secondary mineralization pathways induced by dissimilatory iron reduction of ferrihydrite under advective flow. *Geochim. Cosmochim. Acta* **2003**, *67* (16), 2977−2992.

(36) Katz, J. E.; Zhang, X.; Attenkofer, K.; Chapman, K. W.; Frandsen, C.; Zarzycki, P.; Rosso, K. M.; Falcone, R. W.; Waychunas, G. A.; Gilbert, B. Electron small polarons and their mobility in iron (oxyhydr)oxide nanoparticles. *Science* **2012**, *337* (6099), 1200−1203.

(37) Mikutta, C.; Wiederhold, J. G.; Cirpka, O. A.; Hofstetter, T. B.; Bourdon, B.; Von Gunten, U. Iron isotope fractionation and atom exchange during sorption of ferrous iron to mineral surfaces. *Geochim. Cosmochim. Acta* **2009**, *73* (7), 1795−1812.

(38) Pedersen, H. D.; Postma, D.; Jakobsen, R. Release of arsenic associated with the reduction and transformation of iron oxides. *Geochim. Cosmochim. Acta* **2006**, *70* (16), 4116−4129.

(39) Waychunas, G.; Apted, M.; Brown, G., Jr. X-ray K-edge absorption spectra of Fe minerals and model compounds: Near-edge structure. *Phys. Chem. Minerals* **1983**, *10* (1), 1−9.

(40) *Spectroscopic Methods in Mineralogy*; European Mineralogical Union, 2004; Vol. *6*.

(41) *Spectroscopic Methods in Mineralogy and Material Sciences*; Mineralogical Society of America, 2009; Vol. *78*.

(42) Navrotsky, A. Progress and new directions in high temperature calorimetry revisited. *Phys. Chem. Minerals* **1997**, *24* (3), 222−241.

(43) Beard, B. L.; Johnson, C. M.; Skulan, J. L.; Nealson, K. H.; Cox, L.; Sun, H. Application of Fe isotopes to tracing the geochemical and biological cycling of Fe. *Chem. Geol.* **2003**, *195* (1−4), 87−117.

(44) Arumugam, K.; Becker, U. Computational redox potential predictions: Applications to inorganic and organic aqueous complexes, and complexes adsorbed to mineral surfaces. *Minerals* **2014**, *4* (2), 345−387.

(45) Alexandrov, V.; Neumann, A.; Scherer, M. M.; Rosso, K. M. Electron exchange and conduction in nontronite from first-principles. *J. Phys. Chem. C* **2013**, *117* (5), 2032−2040.

(46) Alexandrov, V.; Rosso, K. M., Electron transport in pure and substituted iron oxyhydroxides by small-polaron migration. *J. Chem. Phys.* **2014**, *140*, (23).

(47) Jordan, D. S.; Hull, C. J.; Troiano, J. M.; Riha, S. C.; Martinson, A. B. F.; Rosso, K. M.; Geiger, F. M. Second harmonic generation studies of Fe(II) interactions with hematite (alpha-Fe₂O₃). *J. Phys. Chem. C* **2013**, *117* (8), 4040−4047.

(48) Kerisit, S.; Rosso, K. M. Computer simulation of electron transfer at hematite surfaces. *Geochim. Cosmochim. Acta* **2006**, *70* (8), 1888−1903.

(49) Rosso, K. M.; Dupuis, M. Electron transfer in environmental systems: A frontier for theoretical chemistry. *Theor. Chem. Acc.* **2006**, *116* (1−3), 124−136.

(50) Becker, U.; Rosso, K. M.; Hochella, M. F. The proximity effect on semiconducting mineral surfaces: A new aspect of mineral surface reactivity and surface complexation theory? *Geochim. Cosmochim. Acta* **2001**, *65* (16), 2641−2649.

(51) Mulvaney, P.; Grieser, F.; Meisel, D., Redox reactions on colloidal metals and metal oxides. In *Kinetics and Catalysis in Microheterogeneous Systems*; Taylor & Francis, Inc., 1991; Vol. *38*, pp 303−373.

(52) Neumann, A.; Hofstetter, T. B.; Lussi, M.; Cirpka, O. A.; Petit, S.; Schwarzenbach, R. P. Assessing the redox reactivity of structural iron in smectites using nitroaromatic compounds as kinetic probes. *Environ. Sci. Technol.* **2008**, *42* (22), 8381−8387.

(53) Chun, C. L.; Penn, R. L.; Arnold, W. A. Kinetic and microscopic studies of reductive transformations of organic contaminants on goethite. *Environ. Sci. Technol.* **2006**, *40* (10), 3299−3304.

(54) Meckstroth, M. L.; Norris, B. J.; Heineman, W. R. Mediator-titrants for thin-layer spectroelectrochemical measurement of bio-component U0′ and n-values. *Bioelectrochem. Bioenerg.* **1981**, *8* (1), 63−70.

(55) Neumann, A.; Hofstetter, T. B.; Skarpeli-Liati, M.; Schwarzenbach, R. P. Reduction of polychlorinated ethanes and carbon tetrachloride by structural Fe(II) in smectites. *Environ. Sci. Technol.* **2009**, *43* (11), 4082−4089.

(56) Neumann, A.; Petit, S.; Hofstetter, T. B. Evaluation of redox-active iron sites in smectites using middle and near infrared spectroscopy. *Geochim. Cosmochim. Acta* **2011**, *75* (9), 2336−2355.

(57) Bylaska, E. J.; Salter-Blanc, A. J.; Tratnyek, P. G. One-electron reduction potentials from chemical structure theory calculations. In *Aquatic Redox Chemistry*; American Chemical Society, 2011; Vol. *1071*, pp 37−64.

(58) Gorski, C. A.; Nurmi, J. T.; Tratnyek, P. G.; Hofstetter, T. B.; Scherer, M. M. Redox behavior of magnetite: Implications for contaminant reduction. *Environ. Sci. Technol.* **2010**, *44* (1), 55−60.

(59) Luan, F.; Gorski, C. A.; Burgos, W. D. Linear free energy relationships for the biotic and abiotic reduction of nitroaromatic compounds. *Environ. Sci. Technol.* **2015**, *49*, 3557−3565.

(60) Pecher, K.; Haderlein, S. B.; Schwarzenbach, R. P. Reduction of polyhalogenated methanes by surface-bound Fe(II) in aqueous suspensions of iron oxides. *Environ. Sci. Technol.* **2002**, *36* (8), 1734−1741.

(61) Grygar, T.; Marken, F.; Schroder, U.; Scholz, F. Electrochemical analysis of solids. A review. *Collect. Czech. Chem. Commun.* **2002**, *67* (2), 163−208.

(62) Scholz, F.; Meyer, B. Electrochemical solid-state analysis—State-of-the-art. *Chem. Soc. Rev.* **1994**, *23* (5), 341−347.

(63) White, A. F.; Peterson, M. L.; Hochella, M. F. Electrochemistry and dissolution kinetics of magnetite and ilmenite. *Geochim. Cosmochim. Acta* **1994**, *58* (8), 1859−1875.

(64) Scholz, F.; Nitschke, L.; Henrion, G.; Damaschun, F. A technique to study the electrochemistry of minerals. *Naturwissenschaften* **1989**, *76* (4), 167−168.

(65) Wang, J. *Analytical Electrochemistry*, 3rd ed.; Wiley-VCH: NJ, 2006.

(66) Hamann, C. H.; Hamnett, A.; Vielstich, W. *Electrochemistry*, 2nd ed.; Wiley-VCH: Weinheim, 2007.

(67) Bard, A. J.; Faulkner, R. F. *Electrochemical methods: Fundamentals and Applications*, 2nd ed.; John Wiley & Sons, Inc.: Hoboken, NJ, 2001.

(68) Rusling, J. F.; Suib, S. L. Characterizing materials with cyclic voltammetry. *Adv. Mater.* **1994**, *6* (12), 922−930.

(69) Kissinger, P. T.; Heineman, W. R. Cyclic voltammetry. *J. Chem. Educ.* **1983**, *60* (9), 702−706.

(70) Domenech-Carbo, A.; Labuda, J.; Scholz, F. Electroanalytical chemistry for the analysis of solids: Characterization and classification (IUPAC Technical Report). *Pure Appl. Chem.* **2013**, *85* (3), 609−631.

(71) Bard, A. J. A life in electrochemistry. *Annu. Rev. Anal. Chem.* **2014**, *7*, 1−21.

(72) Grundl, T. Redox inactivity of colloidal ferric oxyhydroxide solids. *J. Contam. Hydrol.* **1992**, *9*, 369−377.

(73) Shi, Z. Q.; Nurmi, J. T.; Tratnyek, P. G. Effects of nano zero-valent iron on oxidation-reduction potential. *Environ. Sci. Technol.* **2011**, *45* (4), 1586−1592.

(74) Silvester, E.; Charlet, L.; Tournassat, C.; Gehin, A.; Greneche, J. M.; Liger, E. Redox potential measurements and Mössbauer spectrometry of Fe(II) adsorbed onto Fe(III) (oxyhydr)oxides. *Geochim. Cosmochim. Acta* **2005**, *69* (20), 4801−4815.

(75) Morris, J. C.; Stumm, W., Redox equilibria and measurements of potentials in the aquatic environment. In *Equilibrium Concepts in Natural Water Systems*; American Chemical Society, 1967; Vol. *67*, pp 270−285.

(76) Power, G. P.; Ritchie, I. M. Mixed potentials - Experimental illustrations of an important concept in practical electrochemistry. *J. Chem. Educ.* **1983**, *60* (12), 1022−1026.

(77) Tratnyek, P. G.; Macalady, D. L., Oxidation-reduction reactions in the aquatic environment. In *Handbook of Property Estimation Methods for Chemicals*; Boethling, R. S., Ed.; CRC Press: Boca Raton, 2000; pp 383−415.

(78) Balko, B. A.; Clarkson, K. M. The effect of doping with Ti(IV) and Sn(IV) on oxygen reduction at hematite electrodes. *J. Electrochem. Soc.* **2001**, *148* (2), E85−E91.

(79) Cornell, R. M.; Schwertmann, U. *The Iron Oxides: Structure, Properties, Reactions, Occurrence, And Uses*; VCH: New York, 2003.

(80) Larsen, O.; Postma, D. Kinetics of reductive bulk dissolution of lepidocrite, ferrihydrite, and goethite. *Geochim. Cosmochim. Acta* **2001**, *65* (9), 1367−1379.

(81) Postma, D. The reactivity of iron-oxides in sediments—A kinetic approach. *Geochim. Cosmochim. Acta* **1993**, *57* (21−22), 5027−5034.

(82) Laviron, E. Theory of I-t curves at constant potential in case of a solid whose reduction or oxidation is preceded by its dissolution. *J. Electroanal. Chem.* **1978**, *90* (1), 33−47.

(83) Burnham, A. K.; Braun, R. L. Global kinetic analysis of complex materials. *Energy Fuels* **1999**, *13* (1), 1−22.

(84) Vivier, V.; Cachet-Vivier, C.; Mezaille, S.; Wu, B. L.; Cha, C. S.; Nedelec, J. Y.; Fedoroff, M.; Michel, D.; Yu, L. T. Electrochemical Study of Bi_2O_3 and $Bi_2O_2CO_3$ by means of a cavity microelectrode. I. Observed phenomena and direct analysis of results. *J. Electrochem. Soc.* **2000**, *147* (11), 4252−4262.

(85) Grygar, T. Phenomenological kinetics of irreversible electrochemical dissolution of metal-oxide microparticles. *J. Solid State Electrochem.* **1998**, *2* (3), 127−136.

(86) Cachet-Vivier, C.; Vivier, V.; Cha, C. S.; Nedelec, J. Y.; Yu, L. T. Electrochemistry of powder material studied by means of the cavity microelectrode (CME). *Electrochim. Acta* **2001**, *47* (1−2), 181−189.

(87) Fitch, A. Clay-modified electrodes—A review. *Clays Clay Miner.* **1990**, *38* (4), 391−400.

(88) Vago, E. R.; Calvo, E. J.; Stratmann, M. Electrocatalysis of oxygen reduction at well-defined iron-oxide electrodes. *Electrochim. Acta* **1994**, *39* (11−12), 1655−1659.

(89) Shimizu, K.; Boily, J.-F. Electrochemical properties and relaxation times of the hematite/water interface. *Langmuir* **2014**, *30* (31), 9591−9598.

(90) Nurmi, J. T.; Bandstra, J. Z.; Tratnyek, P. G. Packed powder electrodes for characterizing the reactivity of granular iron in borate solutions. *J. Electrochem. Soc.* **2004**, *151* (6), B347−B353.

(91) Cha, C. S.; Li, C. M.; Yang, H. X.; Liu, P. F. Powder Microelectrodes. *J. Electroanal. Chem.* **1994**, *368* (1−2), 47−54.

(92) Haruyama, S.; Masamura, K. The dissolution of magnetite in acidic perchlorate solutions. *Corros. Sci.* **1978**, *18* (4), 263−274.

(93) Nicol, M. J.; Needes, C. R. S. The anodic dissolution of uranium dioxide—I in perchlorate solutions. *Electrochim. Acta* **1975**, *20* (8), 585−589.

(94) Nicol, M. J.; Needes, C. R. S. The anodic dissolution of uranium dioxide—II. In carbonate solutions. *Electrochim. Acta* **1977**, *22* (12), 1381−1384.

(95) Castro, P. A.; Vago, E. R.; Calvo, E. J. Surface electrochemical transformations on spinel iron oxide electrodes in aqueous solutions. *J. Chem. Soc., Faraday Trans.* **1996**, *92* (18), 3371−3379.

(96) Filmer, A.; MacLeod, I.; Parker, A. Oxidation of copper sulfides in aqueous ammonia. II. Electrochemical aspects. *Aust. J. Chem.* **1979**, *32* (5), 975−987.

(97) Mancey, D. S.; Shoesmith, D. W.; Lipkowski, J.; McBride, A. C.; Noel, J. An electrochemical investigation of the dissolution of magnetite in acidic electrolytes. *J. Electrochem. Soc.* **1993**, *140* (3), 637−642.

(98) Yin, Q.; Vaughan, D. J.; England, K. E. R.; Kelsall, G. H. Electrochemical oxidation of covellite (CuS) in alkaline solution. *J. Colloid Interface Sci.* **1994**, *166* (1), 133−142.

(99) Nurmi, J. T.; Tratnyek, P. G. Electrochemical studies of packed iron powder electrodes: Effects of common constituents of natural waters on corrosion potential. *Corros. Sci.* **2008**, *50* (1), 144−154.

(100) Allen, P. D.; Hampson, N. A.; Bignold, G. J. The electrodissolution of magnetite. 2. The oxidation of bulk magnetite. *J. Electroanal. Chem.* **1980**, *111* (2−3), 223−233.

(101) Nurmi, J. T.; Tratnyek, P. G.; Sarathy, V.; Baer, D. R.; Amonette, J. E.; Pecher, K.; Wang, C. M.; Linehan, J. C.; Matson, D. W.; Penn, R. L.; Driessen, M. D. Characterization and properties of metallic iron nanoparticles: Spectroscopy, electrochemistry, and kinetics. *Environ. Sci. Technol.* **2005**, *39* (5), 1221−1230.

(102) Totir, D. A.; Cahan, B. D.; Scherson, D. A. Electrochemical characterization of lithiated transition metal oxide cathode particles in the absence of carbon, binders and other additives. *Electrochim. Acta* **1999**, *45* (1−2), 161−166.

(103) Renock, D.; Mueller, M.; Yuan, K.; Ewing, R. C.; Becker, U. The energetics and kinetics of uranyl reduction on pyrite, hematite, and magnetite surfaces: A powder microelectrode study. *Geochim. Cosmochim. Acta* **2013**, *118* (0), 56−71.

(104) Longhi, M.; Formaro, L. Oxide electrodes. A new technique to bind oxide powders onto Au substrates. *Electrochem. Commun.* **2002**, *4* (2), 123−127.

(105) Scholz, F.; Nitschke, L.; Henrion, G. A new procedure for fast electrochemical analysis of solid materials. *Naturwissenschaften* **1989**, *76* (2), 71−72.

(106) Grygar, T. Kinetics of electrochemical reductive dissolution of Iron(III) hydroxy-oxides. *Collect. Czech. Chem. Commun.* **1995**, *60* (8), 1261−1273.

(107) Grygar, T.; Subrt, J.; Bohacek, J. Electrochemical dissolution of goethite by abrasive stripping voltammetry. *Collect. Czech. Chem. Commun.* **1995**, *60* (6), 950−959.

(108) Grygar, T. The electrochemical dissolution of iron(III) and chromium(III) oxides and ferrites under conditions of abrasive stripping voltammetry. *J. Electroanal. Chem.* **1996**, *405* (1−2), 117−125.

(109) Sharara, Z. Z.; Vittori, O.; Durand, B. Electrochemical reduction of alkaline iron(III) oxides, $LiFeO_2$ and $NaFeO_2$, using carbon paste electrodes. *Electrochim. Acta* **1984**, *29* (12), 1685−1688.

(110) Gruner, W.; Kunath, J.; Kalnishevskaja, L. N.; Posokin, J. V.; Brainina, K. Z. Fundamentals and limitations for the application of the carbon paste electroactive electrode in the electroanalysis of solids. *Electroanalysis* **1993**, *5* (3), 243−250.

(111) Mouhandess, M. T.; Chassagneux, F.; Durand, B.; Sharara, Z. Z.; Vittori, O. Some advantages of carbon paste electrodes in the morphological-study of finely divided iron-oxides. *J. Mater. Sci.* **1985**, *20* (9), 3289−3299.

(112) Mouhandess, M. T.; Chassagneux, F.; Vittori, O. Electrochemical reduction of hematite incorporated in a carbon paste electrode. *C. R. Acad. Sci., Ser. II* **1982**, *294* (10), 571−574.

(113) Mouhandess, M. T.; Chassagneux, F.; Vittori, O. Electrochemical-behavior of alpha-Fe_2O_3 using carbon paste electrodes - influence of particle-size. *J. Electroanal. Chem.* **1982**, *131* (JAN), 367−371.

(114) Sharara, Z. Z.; Vittori, O.; Durand, B. Electrochemical oxidation of divalent iron mixed oxides using carbon paste electrodes. *Electrochim. Acta* **1984**, *29* (12), 1689−1693.

(115) McBreen, J. Electrochemistry of beta-MnO_2 and gamma-MnO_2 in alkaline electrolyte. *Electrochim. Acta* **1975**, *20* (3), 221−225.

(116) Zhang, Z.; Yates, J. T. Band bending in semiconductors: Chemical and physical consequences at surfaces and interfaces. *Chem. Rev.* **2012**, *112* (10), 5520−5551.

(117) Zakharchuk, N.; Meyer, S.; Lange, B.; Scholz, F. A comparative study of lead oxide modified graphite paste electrodes and solid graphite electrodes with mechanically immobilized lead oxides. *Croat. Chem. Acta* **2000**, *73* (3), 667−704.

(118) Ramirez, M. T.; Palomar, M. E.; Gonzalez, I.; Rojashernandez, A. Carbon-paste electrodes with electrolytic binder - influence of the preparation method. *Electroanalysis* **1995**, *7* (2), 184−188.

(119) Kuwana, T.; Heineman, W. R. Study of electrogenerated reactants using optically transparent electrodes. *Acc. Chem. Res.* **1976**, *9* (7), 241−248.

(120) Hawkridg, F. M.; Kuwana, T. Indirect coulometric titration of biological electron-transfer components. *Anal. Chem.* **1973**, *45* (7), 1021−1027.

(121) Szentrimay, R.; Yeh, P.; Kuwana, T., Evaluation of Mediator-tritrants for the indirect coulometric titration of biocomponents. In *Electrochemical Studies of Biological Systems*; Sawyer, D., Ed. ; American Chemical Society: Washington, D.C., 1977; pp 143−169.

(122) Frew, J. E.; Hill, H. A. O. Direct and indirect electron transfer between electrodes and redox proteins. *Eur. J. Biochem.* **1988**, *172* (2), 261−269.

(123) Heineman, W. R.; Hartzell, C. R.; Kuwana, T. Indirect electrochemical titration of beef heart cytochrome C oxidase. *Biochem. Biophys. Res. Commun.* **1972**, *49* (1), 1−&.

(124) Fujihira, Y.; Kuwana, T.; Hartzell, C. R. Reversible redox titrations of cytochrome c and cytochrome c oxidase using detergent solubilized electrochemically generated mediator-titrants. *Biochem. Biophys. Res. Commun.* **1974**, *61* (2), 538−543.

(125) Parker, V. D.; Seefeldt, L. C. A mediated thin-layer voltammetry method for the study of redox protein electrochemistry. *Anal. Biochem.* **1997**, *247* (1), 152−157.

(126) Ito, M.; Kuwana, T. Spectroelectrochemical study of indirect reduction of triphosphopyridine nucleotide. 1. Methyl viologen, ferredoxin-TPN-reductase and TPN. *J. Electroanal. Chem.* **1971**, *32* (3), 415−&.

(127) Watt, G. D. An electrochemical method for measuring redox potentials of low potential proteins by microcoulometry at controlled potentials. *Anal. Biochem.* **1979**, *99* (2), 399−407.

(128) Watt, G. D.; Frankel, R. B.; Papaefthymiou, G. C. Reduction of mammalian ferritin. *Proc. Natl. Acad. Sci. U.S.A.* **1985**, *82* (11), 3640−3643.

(129) Chasteen, N. D.; Ritchie, I. M.; Webb, J. Stepped potential microcoulometry of ferritin. *Anal. Biochem.* **1991**, *195* (2), 296−302.

(130) Spence, J. T.; Barber, M. J.; Siegel, L. M. Determination of the stoichiometry of electron uptake and the midpoint reduction potentials of milk xanthine-oxidase at 25 degrees C by micro-coulometry. *Biochemistry* **1982**, *21* (7), 1656−1661.

(131) Watt, G. D.; Burns, A.; Lough, S.; Tennent, D. L. Redox and spectroscopic properties of oxidized mofe protein from azotobacter-vinelandii. *Biochemistry* **1980**, *19* (21), 4926−4932.

(132) Baron, D.; LaBelle, E.; Coursolle, D.; Gralnick, J. A.; Bond, D. R. Electrochemical measurement of electron transfer kinetics by *Shewanella oneidensis* MR-1. *J. Biol. Chem.* **2009**, *284* (42), 28865−28873.

(133) Coursolle, D.; Baron, D. B.; Bond, D. R.; Gralnick, J. A. The Mtr respiratory pathway is essential for reducing flavins and electrodes in *Shewanella oneidensis*. *J. Bacteriol.* **2010**, *192* (2), 467−474.

(134) Marsili, E.; Baron, D. B.; Shikhare, I. D.; Coursolle, D.; Gralnick, J. A.; Bond, D. R. *Shewanella* secretes flavins that mediate extracellular electron transfer. *Proc. Natl. Acad. Sci. U.S.A.* **2008**, *105* (10), 3968−3973.

(135) Mehta-Kolte, M. G.; Bond, D. R. *Geothrix fermentans* secretes two different redox-active compounds to utilize electron acceptors across a wide range of redox potentials. *Appl. Environ. Microbiol.* **2012**, *78* (19), 6987−6995.

(136) O'Loughlin, E. J. Effects of electron transfer mediators on the bioreduction of lepidocrocite (gamma-FeOOH) by Shewanella putrefaciens CN32. *Environ. Sci. Technol.* **2008**, *42* (18), 6876−6882.

(137) Okamoto, A.; Hashimoto, K.; Nealson, K. H.; Nakamura, R. Rate enhancement of bacterial extracellular electron transport involves bound flavin semiquinones. *Proc. Natl. Acad. Sci. U.S.A.* **2013**, *110* (19), 7856−7861.

(138) Kotloski, N. J.; Gralnick, J. A., Flavin electron shuttles dominate extracellular electron transfer by *Shewanella oneidensis*. *Mbio* **2013**, *4*, (1).

(139) Lovley, D. R.; Fraga, J. L.; Blunt-Harris, E. L.; Hayes, L. A.; Phillips, E. J. P.; Coates, J. D. Humic substances as a mediator for microbially catalyzed metal reduction. *Acta Hydrochim. Hydrobiol.* **1998**, *26* (3), 152−157.

(140) Lovley, D. R.; Coates, J. D.; BluntHarris, E. L.; Phillips, E. J. P.; Woodward, J. C. Humic substances as electron acceptors for microbial respiration. *Nature* **1996**, *382* (6590), 445−448.

(141) Kappler, A.; Benz, M.; Schink, B.; Brune, A. Electron shuttling via humic acids in microbial iron(III) reduction in a freshwater sediment. *FEMS Microbiol. Ecol.* **2004**, *47* (1), 85−92.

(142) Shen, Z. H.; Parker, V. D.; Aust, A. E. Mediated, thin-layer cell, coulometric determination of redox-active iron on the surface of asbestos fibers. *Anal. Chem.* **1995**, *67* (2), 307−311.

(143) Tratnyek, P. G.; Wolfe, N. L. Characterization of the reducing properties of anaerobic sediment slurries using redox indicators. *Environ. Toxicol. Chem.* **1990**, *9* (3), 289−295.

(144) Tratnyek, P. G.; Reilkoff, T. E.; Lemon, A. W.; Scherer, M. M.; Balko, B. A.; Feik, L. M.; Henegar, B. D. Visualizing redox chemistry: Probing environmental oxidation−reduction reactions with indicator dyes. *Chem. Educ.* **2001**, *6*, 172−179.

(145) Orsetti, S.; Laskov, C.; Haderlein, S. B. Electron transfer between iron minerals and quinones: Estimating the reduction potential of the Fe(II)-goethite surface from AQDS speciation. *Environ. Sci. Technol.* **2013**, *47* (24), 14161−14168.

(146) Klein, A. R.; Silvester, E.; Hogan, C. F. Mediated electron transfer between Fe-II adsorbed onto hydrous ferric oxide and a working electrode. *Environ. Sci. Technol.* **2014**, *48* (18), 10835−10842.

(147) Gorski, C. A.; Aeschbacher, M.; Soltermann, D.; Voegelin, A.; Baeyens, B.; Fernandes, M. M.; Hofstetter, T. B.; Sander, M. Redox properties of structural Fe in clay minerals. 1. Electrochemical quantification of electron-donating and -accepting capacities of smectites. *Environ. Sci. Technol.* **2012**, *46* (17), 9360−9368.

(148) Gorski, C. A.; Klupfel, L.; Voegelin, A.; Sander, M.; Hofstetter, T. B. Redox properties of structural Fe in clay minerals. 2. Electrochemical and spectroscopic characterization of electron transfer irreversibility in ferruginous smectite, SWa-1. *Environ. Sci. Technol.* **2012**, *46* (17), 9369−9377.

(149) Gorski, C. A.; Klüpfel, L.; Voegelin, A.; Sander, M.; Hofstetter, T. B. Redox properties of structural Fe in clay minerals: 3. Relationships between smectite redox and structural properties. *Environ. Sci. Technol.* **2013**, *47* (23), 13477−13485.

(150) Aeschbacher, M.; Brunner, S. H.; Schwarzenbach, R. P.; Sander, M. Assessing the effect of humic acid redox state on organic pollutant sorption by combined electrochemical reduction and sorption experiments. *Environ. Sci. Technol.* **2012**, *46* (7), 3882−3890.

(151) Aeschbacher, M.; Graf, C.; Schwarzenbach, R. P.; Sander, M. Antioxidant properties of humic substances. *Environ. Sci. Technol.* **2012**, *46* (9), 4916−4925.

(152) Aeschbacher, M.; Sander, M.; Schwarzenbach, R. P. Novel electrochemical approach to assess the redox properties of humic substances. *Environ. Sci. Technol.* **2010**, *44* (1), 87−93.

(153) Aeschbacher, M.; Vergari, D.; Schwarzenbach, R. P.; Sander, M. Electrochemical analysis of proton and electron transfer equilibria of the reducible moieties in humic acids. *Environ. Sci. Technol.* **2011**, *45* (19), 8385−8394.

(154) Gulkowska, A.; Sander, M.; Hollender, J.; Krauss, M. Covalent binding of sulfamethazine to natural and synthetic humic acids: Assessing laccase catalysis and covalent bond stability. *Environ. Sci. Technol.* **2013**, *47* (13), 6916−6924.

(155) Kluepfel, L.; Keiluweit, M.; Kleber, M.; Sander, M. Redox properties of plant biomass-derived black carbon (biochar). *Environ. Sci. Technol.* **2014**, *48* (10), 5601−5611.

(156) Kluepfel, L.; Piepenbrock, A.; Kappler, A.; Sander, M. Humic substances as fully regenerable electron acceptors in recurrently anoxic environments. *Nature Geoscience* **2014**, *7* (3), 195−200.

(157) Stone, A. T.; Morgan, J. J. Reduction and dissolution of manganese(III) and manganese(IV) oxides by organics. 1. Reaction with hydroquinone. *Environ. Sci. Technol.* **1984**, *18* (6), 450−456.

(158) Vuorilehto, K. Stable, colourless and water-soluble electron-transfer mediators used in enzyme electrochemistry. *J. Appl. Electrochem.* **2008**, *38* (10), 1427−1433.

(159) Swearingen, C.; Wu, J.; Stucki, J.; Fitch, A. Use of ferrocenyl surfactants of varying chain lengths to study electron transfer reactions in native montmorillonite clay. *Environ. Sci. Technol.* **2004**, *38* (21), 5598−5603.

(160) Kulys, J.; Buchrasmussen, T.; Bechgaard, K.; Razumas, V.; Kazlauskaite, J.; Marcinkeviciene, J.; Christensen, J. B.; Hansen, H. E. Study of the new electron-transfer mediators in glucose-oxidase catalysis. *J. Mol. Catal.* **1994**, *91* (3), 407−420.

(161) Sakamoto, T.; Ohsako, T.; Matsuo, T.; Mulac, W. A.; Meisel, D. Pulse-radiolysis studies of electron-transfer between polymer and zwitterionic viologen radicals. *Chem. Lett.* **1984**, No. 11, 1893−1896.

(162) Roller, S. D.; Bennetto, H. P.; Delaney, G. M.; Mason, J. R.; Stirling, J. L.; Thurston, C. F. Electron-transfer coupling in microbial fuel-cells 0.1. Comparison of redox-mediator reduction rates and respiratory rates of bacteria. *J. Chem. Technol. Biotechnol., Biotechnol.* **1984**, *34* (1), 3−12.

(163) Delaney, G. M.; Bennetto, H. P.; Mason, J. R.; Roller, S. D.; Stirling, J. L.; Thurston, C. F. Electron-transfer coupling in microbial fuel-cells 0.2. Performance of fuel-cells containing selected micro-organism mediator substrate combinations. *J. Chem. Technol. Biotechnol., Biotechnol.* **1984**, *34* (1), 13−27.

(164) Prince, R. C.; Linkletter, S. J. G.; Dutton, P. L. The thermodynamic properties of some commonly used oxidation-reduction mediators, inhibitors and dyes, as determined by polarography. *Biochim. Biophys. Acta* **1981**, *635* (1), 132−148.

(165) Michaelis, L.; Eagle, H. Some redox indicators. *J. Biol. Chem.* **1930**, *87* (3), 713−727.

(166) Fultz, M. L.; Durst, R. A. Mediator compounds for the electrochemical study of biological redox systems—A compilation. *Anal. Chim. Acta* **1982**, *140* (1), 1−18.

(167) Szentrimay, R.; Yeh, P.; Kuwana, T., Evaluation of mediator-titrants for the indirect coulometric titration of biocomponents. In *Electrochemical Studies of Biological Systems*; Sawyer, D. T., Ed.; American Chemical Society: Washington, DC, 1977; pp 143−169.

(168) Wenk, J.; Aeschbacher, M.; Salhi, E.; Canonica, S.; von Gunten, S.; Sander, M. Chemical oxidation of dissolved organic matter by chlorine dioxide, chlorine, and ozone: Effects on its optical and antioxidant properties. *Environ. Sci. Technol.* **2013**, *47* (19), 11147−11156.

(169) Page, S. E.; Sander, M.; Arnold, W. A.; McNeill, K. Hydroxyl radical formation upon oxidation of reduced humic acids by oxygen in the dark. *Environ. Sci. Technol.* **2012**, *46* (3), 1590−1597.

(170) Sharpless, C. M.; Aeschbacher, M.; Page, S. E.; Wenk, J.; Sander, M.; McNeill, K. Photooxidation-induced changes in optical, electrochemical, and photochemical properties of humic substances. *Environ. Sci. Technol.* **2014**, *48* (5), 2688−2696.

(171) Page, S. E.; Kling, G. W.; Sander, M.; Harrold, K. H.; Logan, J. R.; McNeill, K.; Cory, R. M. Dark formation of hydroxyl radical in arctic soil and surface waters. *Environ. Sci. Technol.* **2013**, *47* (22), 12860−12867.

(172) Lau, M.; Sander, M.; Gelbrecht, J.; Hupfer, M. Solid phases as important electron acceptors in freshwater organic sediments. *Biogeochemistry* **2015**, *123*, 49−61.

(173) Amonette, J. E.; Templeton, J. C. Improvements to the quantitative assay of nonrefractory minerals for Fe(II) and total Fe using 1,10-phenanthroline. *Clays Clay Miner.* **1998**, *46* (1), 51−62.

(174) Stucki, J. W.; Golden, D. C.; Roth, C. B. Preparation and handling of dithionite-reduced smectite suspensions. *Clays Clay Miner.* **1984**, *32* (3), 191−197.

(175) Drits, V. A.; Manceau, A. A model for the mechanism of Fe^{3+} to Fe^{2+} reduction in dioctahedral smectites. *Clays Clay Miner.* **2000**, *48* (2), 185−195.

(176) Lear, P. R.; Stucki, J. W. Role of structural hydrogen in the reduction and reoxidation of iron in nontronite. *Clays Clay Miner.* **1985**, *33* (6), 539−545.

(177) Favre, F.; Stucki, J. W.; Boivin, P. Redox properties of structural Fe in ferruginous smectite. A discussion of the standard potential and its environmental implications. *Clays Clay Miner.* **2006**, *54* (4), 466−472.

(178) Hadi, J.; Tournassat, C.; Ignatiadis, I.; Greneche, J. M.; Charlet, L. Modelling CEC variations versus structural iron reduction levels in dioctahedral smectites. Existing approaches, new data and model refinements. *J. Colloid Interface Sci.* **2013**, *407* (0), 397−409.

(179) Neumann, A.; Sander, M.; Hofstetter, T. B. Redox properties of structural Fe in smectite clay minerals. In *Aquatic Redox Chemistry*, Tratnyek, P. G.; Grundl, T.; Haderlein, S., Eds.; American Chemical Society, 2011; Vol. *1071*, pp 361−379.

(180) Mulvaney, P.; Swayambunathan, V.; Grieser, F.; Meisel, D. Dynamics of interfacial charge-transfer in iron(III) oxide colloids. *J. Phys. Chem.* **1988**, *92* (23), 6732−6740.

(181) Amemiya, S., Scanning electrochemical microscopy. In *Characterization of Materials*, 2nd ed.; John Wiley & Sons, Inc., 2012; pp 1−13.

(182) Bard, A. J.; Denuault, G.; Lee, C.; Mandler, D.; Wipf, D. O. Scanning electrochemical microscopy—A new technique for the characterization and modification of surfaces. *Acc. Chem. Res.* **1990**, *23* (11), 357−363.

(183) Bard, A. J.; Mirkin, M. V. *Scanning Electrochemical Microscopy.* 2nd ed.; CRC Press: Boca Raton, FL, 2012.

2   **Electrochemical analyses of redox-active iron minerals:**

3   **A review of non-mediated and mediated approaches**

4   Michael Sander,[1,*] Thomas B. Hofstetter,[2] and Christopher A. Gorski,[3,*]

5   1: Department of Environmental Systems Science, Institute of Biogeochemistry and

6   Pollutant Dynamics, Environmental Chemistry, Swiss Federal Institute of Technology

7   (ETH), Universitätstrasse 16, 8092 Zurich

8   email: michael.sander@env.ethz.ch

9   2: Environmental Chemistry; Swiss Federal Institute of Aquatic Science and

10   Technology (Eawag); Ueberlandstrasse 133; 8600 Duebendorf; Switzerland

11

12   3: Civil and Environmental Engineering, The Pennsylvania State University, 212

13   Sackett Building. University Park, PA 16802-1408, USA

14   email: gorski@engr.psu.edu

15   Submitted as critical review to *Environmental Science & Technology*

16

17   Corresponding authors

18

19   Phone & Fax numbers of corresponding authors:
20   Michael Sander:
21   Phone: +41 (0)44 632-8314
22   Fax: +41 (0)44 633-1122
23   Christopher A. Gorski
24   Phone: +1 (814) 865-5673
25   Fax: +1 (814) 863-7304

26

Detailed description of mediated amperometric and potentiometric measurements

The following subsections provide a detailed description of the electrochemical cell setups used in mediated amperometric and potentiometric measurements of mineral species. These measurements are almost always sensitive to O_2 and therefore have to be carried out under anoxic conditions. While anoxic conditions can be established by purging the electrochemical cell solution and the samples with N_2 or Ar before and during the analysis, it may be more convenient to carry out the measurements in an anoxic glove box.

In principle, mediated electrochemical analysis can be applied to minerals that are immobilized on the working electrode surface or suspended in the solution of the electrochemical cell (see **Figure 1** in the manuscript). The subsequent discussion will focus on the analysis of suspended minerals because of several advantages of this approach. First, the analysis of suspended minerals is comparatively fast and facile because no immobilization of the mineral on the working electrode surface is required. Second, the use of bare, unmodified working electrodes eliminates potential experimental artifacts associated with the immobilization procedure of the mineral. Third, a precise amount of mineral can be added to the electrochemical cell. This is a prerequisite when quantifying the dependence of the extents of reduction or oxidation of the mineral on the applied reduction potential E and the solution pH.

Cell setup for mediated amperometric measurements

As detailed in the manuscript, amperometric measurements are conducted in electrochemical cells containing three electrodes. We have in the past successfully used cells with working electrodes made out of vitreous carbon (sources: Bioanalytical Systems, Inc. and ALS Co., Ltd) and glassy carbon (Sigradur G® from HTW Hochtemperatur-Werkstoffe GmbH) working electrodes,[1-3] Pt wire counter electrodes, and Ag/AgCl reference electrodes. We used carbonaceous working electrode materials because they can be polarized over a wide E_H range from approximately -1.2 V to +1.0 V [4] without reducing protons or oxidizing water, respectively. In comparison, metal electrodes typically have narrower E_H ranges (*e.g.*, approximately -0.7 to +1.0 V for platinum), mainly due to much smaller overpotentials for H^+ reduction at reducing E_H values.[4] The counter electrode is positioned in a counter electrode glass compartment that is connected to the working

59 electrode compartment by a porous glass frit (or a membrane). The frit serves to

60 minimize (or even fully eliminate) mass transfer of both the mineral and the mediator

61 species from the working electrode to the counter electrode at which the mineral and

62 the analyte would undergo unwanted electron transfer reactions. The electrochemical

63 cell is continuously stirred either by using an overhead stirrer or a magnetic stirrer

64 during the analysis to ensure mixing of the mineral and the mediator and fast mass

65 transfer of the mediator to and from the mineral and working electrode surfaces.

66   The electrochemical cell is filled with an electrolyte solution containing a pH

67 buffer that, itself, is redox-inactive and that does not specifically interact with the

68 working electrode or the mineral. A constant defined potential E is then applied to the

69 working electrode using a potentiostat. Because there are no electro-active species in

70 the cell solution at this point, the initial measured currents are small and result from

71 charging/discharging of the working electrode-solution interface. Subsequent addition

72 of the redox mediator to the working electrode compartment results in reductive and

73 oxidative current responses in the form of current peaks: initial reduction/oxidation of

74 a large number of the added mediator molecules per time result in high initial

75 currents, which subsequently decrease as the reduction potential of the mediator in

76 solution approaches the E applied to the working electrode. The current levels off at

77 stable and low values when redox equilibrium is attained between the electrode and

78 mediator species in solution. To ensure proper redox mediation in the subsequent

79 steps, the applied E should be within ± 120 mV of the mediator's apparent standard

80 reduction potential, $E_H^{0'}$, under the given experimental conditions. Beyond this range,

81 E_H values becomes difficult to control and accurately measure, for the same reason

82 that a pH buffer functions only near its pKa value. Note that the mediator may be

83 added in excess relative to the amount of analyte that is added in subsequent steps.

84   Following attainment of redox equilibrium of the mediator with the working

85 electrode, the mineral is added to the working electrode compartment. Redox non-

86 equilibrium between the mineral and the mediator triggers electron transfer between

87 them. As a consequence, the mediator speciation changes and, to re-attain redox

88 equilibrium with the working electrode, the mediator is reduced or oxidized, resulting

89 in a reductive or oxidative current response, respectively. For instance, assume a

90 diquat-mediated electrochemical reduction of a Fe^{3+}-bearing mineral under reducing

91 E_H conditions (see **Figure 2c** in the manuscript). The reduced diquat species ($DQ^{\bullet+}$)

92 reduces the ferric iron (Fe^{3+}) to form ferrous iron (Fe^{2+}) and the oxidized diquat

93   species (DQ^{2+}). This reaction increases the ratio of DQ^{2+} to $DQ^{\bullet+}$ and therefore the

94   reduction potential of the solution, $E_{solution}$, above the reduction potential applied to

95   the working electrode, $E_{applied}$. To re-establish redox equilibrium, $DQ^{\bullet+}$ molecules are

96   re-reduced at the working electrode, resulting in a reductive current peak. Upon

97   attainment of redox (E) equilibrium between the mineral (or its dissolved product

98   species) and the mediator, new analyte may be added to the cell for analysis. It is

99   important to note that the addition of a mineral to an electrochemical cell with a

100 reducing applied E may also result in an oxidative current response. This would be the

101 case if the mineral has a lower reduction potential than the E value applied to the

102 working electrode and hence the mediator in solution. For example, iron minerals

103 containing Fe^{2+} may have sufficiently low reduction potentials to reduce DQ^{2+} to

104 $DQ^{\bullet+}$, which is then re-oxidized at the working electrode. Mediated electrochemical

105 oxidation proceeds in an analogous manner to mediated electrochemical reduction

106 (see **Figure 2c** in the manuscript). For example, a mineral containing Fe^{2+} may reduce

107 the oxidant $ABTS^{\bullet+}$ to ABTS, which then is re-oxidized at the working electrode,

108 resulting in an oxidative current peak.

109 ***Cell setup for mediated OCP measurements***

110 Potentiometric measurements are often conducted with combined redox electrodes

111 that contain the working electrode (*e.g.*, a platinum ring) and the reference electrode

112 (*e.g.*, Ag/AgCl) in a single enclosure. Potentiometric measurements are easily

113 conducted by simply submerging a calibrated redox electrode into an aqueous

114 solution containing the suspended mineral. Under continuous stirring, the open circuit

115 potential, E^{OCP}, is monitored over time. In the absence of redox mediators M, E^{OCP}

116 values are affected by the measurement conditions (*e.g.*, the stirring speed) and drift

117 over time, reflecting redox non-equilibrium between the working electrode and the

118 suspended mineral [5]. Addition of one or more redox mediator(s) facilitates attainment

119 of redox (E) equilibrium and is expected to result in quick stabilization of E^{OCP}

120 values. Facilitated redox equilibration has previously been demonstrated for mediated

121 potentiometric measurements of natural organic matter at different redox states.[2, 6]

122 While the use of redox mediator helps overcome the challenge of redox non-

123 equilibriums in potentiometric measurements, care must be taken when deciding

124 which mediator is used and how much the mediator is added to rule out measurement

125 artifacts. First, to ensure reliable potentiometric measurements, the (expected) E of the

126   mineral needs to fall into the $E_H^{0'}$ range of the mediator $\pm$ 120 mV. A list of suitable

127   redox mediators is provided in the manuscript (see **Figure 3** in the manuscript). The

128   reduction potential of the mineral analyte therefore determines which mediators are

129   suitable. Potentiometric measurements in which the final E^{OCP} values are below or

130   above the redox buffering range of the mediator need to be repeated with a mediator

131   with a lower or higher $E_H^{0'}$, respectively. Second, the mediator needs to be added in

132   amounts that are sufficiently large to ensure proper mediation but — at the same time

133   — sufficiently small to not alter the redox state of the mineral upon E equilibration.

134   The addition of large amounts of the mediator may causes significant oxidation or

135   reduction of the mineral and may thereby alter its redox state and hence reduction

136   potential. The number of mediator molecules therefore must be much smaller than the

137   number of electrons that are accepted or donated by the mineral. It is important to

138   note that the "open circuit" in mediated potentiometric measurements only impairs

139   electron transfer to and from the working electrode but not between the mineral and

140   the added mediator.

141

142   ***Kinetic analysis of current responses***

143   This section provides a detailed derivation of Equation 10 in the manuscript that

144   relates the measured current I (units [A= C/s]) to the rate of electron transfer between

145   a mediator and a redox-active element in a mineral. For illustrative purposes, the

146   subsequent derivation is carried out for the reductive current response I in mediated

147   electrochemical reduction (MER) in response to the addition of a Fe^{3+}-containing

148   mineral to the electrochemical cell. We assume that the addition of the mineral does

149   not alter the volume of the solution in the cell and hence the concentration of the

150   reduced mediator and the surface area of the WE over which electrons are transferred.

151   At any given time during MER, the background-corrected reductive current

152   response I corresponds to the instantaneous rate at which electrons are transferred

153   from the reduced mediator to electroactive Fe^{3+} in the mineral and hence the rate at

154   which the electroactive Fe^{3+} is converted to Fe^{2+}, assuming that Fe^{3+} reduction is the

155   rate-limiting step:

156   $$I = F \cdot \frac{dn_{e-}}{dt} = -F \cdot \frac{dn_{Fe3+}}{dt} = F \cdot \frac{dn_{Fe2+}}{dt}$$ **Eq. S1**

157   where F is the Faraday constant (= 96485 [C/mol]), n_{e-} [mol electrons] and n_{Fe3+} and

158 n_{Fe2+} (both [mol iron]) are the number of electrons transferred and the number of Fe^{3+}

159 converted to Fe^{2+}, respectively.

160   Assuming that the electron transfer from the reduced mediator to mineral-

161 associated electroactive Fe^{3+} follows a second order rate law, the rate of Fe^{3+}

162 reduction can also be expressed as:

163      $$\frac{d[Fe^{3+}]}{dt} = k_{ET} \cdot [Fe^{3+}] \cdot [M_{red}]$$ **Eq. S2**

164 where k_{ET} [mol L^{-1} s^{-1}] is the second order rate constant of electron transfer from the

165 reduced mediator to mineral–associated electroactive Fe^{3+}, $[Fe^{3+}]$ (in [mol$_{Fe}$ L^{-1}])

166 and $[M_{red}]$ (in [mol $_{Mred}$ L^{-1}]) are the concentrations of electroactive Fe^{3+} and reduced

167 mediator, M_{red}, in the electrochemical cell. We note that the concentration of

168 electroactive Fe^{3+} may be smaller than the total concentration of Fe^{3+} in cases that the

169 mineral contains Fe^{3+} that cannot be reduced under the given MER conditions.

170   Integration of Eq. S2 yields:

171      $$[Fe^{3+}(t)] = [Fe^{3+}(t_0)] \cdot e^{-k_{ET} \cdot [M_{red}] \cdot t}$$ **Eq. S3**

172   where $[Fe^{3+}(t)]$ and $[Fe^{3+}(t_0)]$ are the concentrations of mineral-associated

173 electroactive Fe^{3+} at time t during the reduction and at time t_0 at the onset of the

174 reduction, respectively.

175   The concentration of electroactive Fe^{3+} at a given time t can also be expressed in

176 terms of a mass balance on Fe in the MER system (note that the solution volume in

177 the electrochemical cell is constant during MER):

178      $$[Fe^{3+}(t)] = [Fe^{3+}(t_0)] - [Fe^{2+}(t)]$$ **Eq. S4**

179   where $[Fe^{2+}(t)]$ [mol Fe^{2+} L^{-1}] is the concentration of Fe^{2+} formed in the system

180 by mediated electrochemical reduction from the onset of the reduction to time t.

181   It is possible to express Eq. S4 also in the form of current integrals:

182      $$[Fe^{3+}(t)] = \frac{\int_{t_0}^{t\infty}\left(\frac{1}{F} \cdot I(t)\right)dt - \int_{t_0}^{t}\left(\frac{1}{F} \cdot I(t)\right)dt}{V}$$ **Eq. S5**

183   where V [L] is the solution volume in the electrochemical cell, t_∞ [s] is the time at

184 which all electroactive Fe^{3+} has been reduced during MER and I(t) [A] is the
185 background-corrected reductive current response at time t. The two integral terms on
186 the right of Equation S5 correspond to $[Fe^{3+}(t_0)] - [Fe^{2+}(t)]$.

187 Combining equations S3 and S5 yields:

188 $$\int_{t_0}^{t_\infty} \left(\frac{1}{F} \cdot I(t) \right) dt - \int_{t_0}^{t} \left(\frac{1}{F} \cdot I(t) \right) dt = \int_{t_0}^{t_\infty} \left(\frac{1}{F} \cdot I(t) \right) dt \cdot e^{-k_{ET} \cdot [M_{red}] \cdot t} \quad \textbf{Eq. S6}$$

189 which can be re-arranged to:

190 $$-k_{ET} \cdot [M_{red}] \cdot t = \ln \left(1 - \frac{\int_{t_0}^{t} \left(\frac{1}{F} \cdot I(t) \right) dt}{\int_{t_0}^{t_\infty} \left(\frac{1}{F} \cdot I(t) \right) dt} \right) \quad \textbf{Eq. S7}$$

191 The concentration of the reduced mediator, $[M_{red}]$, remains constant during the
192 MER (because the reduced mediator is constantly regenerated at the WE) and can be
193 determined by integration of the mediator current peak at the onset of the MER:

194 $$[M_{red}] = \frac{\int_{t_{0\_M}}^{t_{\infty\_M}} \left(\frac{1}{F} \cdot I_M(t) \right) dt}{V} \quad \textbf{Eq. S8}$$

195 where t_{0_M} and t_{∞_M} (both [s]) are the times at which the mediator is added to the

196 electrochemical cell and at which the mediator is in equilibrium with the potential
197 applied to the WE, and I_M(t) [C] is the background-corrected current response at time
198 t due to the reduction of the mediator.
199 The rate constant of electron transfer from the reduced mediator to electroactive

200 Fe^{3+} can then be extracted from the slope of a regression line of $\ln \left(1 - \frac{\int_{t_0}^{t} \left(\frac{1}{F} \cdot I(t) \right) dt}{\int_{t_0}^{t_\infty} \left(\frac{1}{F} \cdot I(t) \right) dt} \right)$

201 versus t. Systems in which the electron transfer to the electroactive Fe^{3+} during MER
202 accelerates or decelerates would result in increasing and decreasing slopes,
203 respectively.
204

205 **References**

206 1.   Aeschbacher, M.; Sander, M.; Schwarzenbach, R. P., Novel Electrochemical
207 Approach to Assess the Redox Properties of Humic Substances. *Environmental*
208 *Science & Technology* **2010,** *44*, (1), 87-93.
209 2.   Aeschbacher, M.; Vergari, D.; Schwarzenbach, R. P.; Sander, M.,
210 Electrochemical Analysis of Proton and Electron Transfer Equilibria of the Reducible
211 Moieties in Humic Acids. *Environmental Science & Technology* **2011,** *45*, (19), 8385-

212   8394.

213   3.   Kluepfel, L.; Keiluweit, M.; Kleber, M.; Sander, M., Redox Properties of Plant
214   Biomass-Derived Black Carbon (Biochar). *Environmental Science & Technology*
215   **2014,** *48*, (10), 5601-5611.

216   4.   Bard, A. J.; Faulkner, R. F., *Electrochemical methods: fundamentals and*
217   *applications*. 2nd ed.; John Wiley & Sons, Inc.: Hoboken, NJ, 2001.

218   5.   Shi, Z. Q.; Nurmi, J. T.; Tratnyek, P. G., Effects of Nano Zero-Valent Iron on
219   Oxidation-Reduction Potential. *Environmental Science & Technology* **2011,** *45*, (4),
220   1586-1592.

221   6.   Klupfel, L.; Piepenbrock, A.; Kappler, A.; Sander, M., Humic substances as
222   fully regenerable electron acceptors in recurrently anoxic environments. *Nature*
223   *Geoscience* **2014,** *7*, (3), 195-200.

224